Theoretical optimizations of quantum repeaters based on atomic ensembles

MSc in Physics, 2021-2022

Camilla Birch Okkels

Supervisor:

Anders Søndberg Sørensen

University of Copenhagen

Faculty:	Faculty of Science
Institute:	The Niels Bohr Institute
Author:	Camilla Birch Okkels KU-ID: nrp376
Title:	Theoretical optimizations of quantum repeaters based on atomic ensembles
Supervisor:	Anders Søndberg Sørensen anders.sorensen@nbi.ku.dk
Handed in:	June, 2022

UNIVERSITY OF
COPENHAGEN

Acknowledgements

I would like express my deepest appreciation to my supervisor Anders Søndberg Sørensen for his guidance in writing this thesis. Without his help in understanding the material and keeping an eye on the direction of the project during writing this project would surely not have been possible.

Another special thanks to Post Doc. Yuxiang Zhang. Not just for providing technical support to understand how to run simulations of the protocols, but also for answering questions about the material in general.

Abstract

Quantum repeaters are a solution to the problem of sending quantum information over long distances. They take advantage of entanglement and using so-called swapping processes to distribute entanglement. This thesis explores the effect of imperfections on quantum repeater protocols. A particular imperfection this thesis focuses on exploring is the multi-photon error arising from a photon source having a probability of emitting more than one photon. Imperfections greatly reduce the efficiency and accuracy of repeater protocols. To mitigate the effect of imperfections more advanced repeater protocols can be thought of that are more robust e.g. the two-click swapping schemes compared to the simpler one-click swapping scheme. Two protocols are introduced. The Jiang protocol using the one-click entanglement generation, one type of two-click swap for the first swapping and a second type of two-click swap for all subsequent swaps. The second protocol is a modified version using one-click entanglement generation and the first type of two-click swapping for all swaps. Comparing the two protocols the modified version proved more robust towards imperfections. This was due to a higher fidelity of the final state.

Contents

1 Introduction

Quantum mechanics has always been one of the more counterintuitive fields in physics. It aims to describe our world on atomic and subatomic levels, and its probabilistic nature seems very different from the deterministic behaviours we can observe from large scale systems. Heisenberg's uncertainty principle and entanglement are just some of the strange consequences that arise from the axioms of quantum mechanics.
An effect of interest to this thesis is the no-cloning theorem[1]. Due to this effect, the classical solution to allow for long-distance communication is not possible. When transmitting a signal in fiber optic cables a big problem is loss of photons as they get absorbed in the fiber. To deal with this classically repeater nodes are inserted in between the sender and receiver and thereby divides the distance in smaller sections. These repeaters measure the incoming signal. Several copies of the signal are then re-transmitted. Quantum repeaters also divide the distance in smaller sections by inserting repeater nodes. Unfortunately, due to the no-cloning theorem an unknown quantum state can not be copied. Instead quantum repeaters make use of entanglement and entanglement swapping which would theoretically allow transmission of quantum information over long distances.

While repeaters work great theoretically, reality is that repeater protocols are challenged by a number of different imperfections such as photon loss, detector efficiency and dark counts. If the photon source used in the repeater protocol has a probability of emitting more than one photon[2] it also creates an increased risk of multi-photon errors. Of course multi-photon errors would not be a problem for number resolving detectors if there were no other imperfections, but this is not realistic. To have a more realistic representation of the performance of a quantum repeater protocol the effect of imperfections must be included.

The focus of this thesis will be to explore the efficiency and accuracy of repeater protocols given we can neglect or just suppress the term that has the ensembles emitting two photons. This is motivated by the fact that it has been shown it is possible to create such a state [1]. For this reason it is interesting to explore exactly the value of decreasing or completely removing this particular multi-photon error. The ultimate goal is to explore how to get closer to a repeater protocol which can actually be used in a real communication system.

This thesis will explore quantum repeater protocols. It will calculate how they work using simple protocols with ideal states and without imperfections. Imperfections will then be introduced and some more advanced protocols designed to mitigate the effects of imperfections will be described. Simulations will be run to compare the performance of different repeater protocols

[1] See proof in chapter 3.1.1

[2] The probability of emitting more than two photons is however very small and can be disregarded. In this paper we will only be concerned with the term that has the ensemble emitting two photons.

under varying conditions. This will also illustrate the effect of different imperfections on the protocols.

Lastly it has been shown that it is possible to create the photon-number entangled state $\alpha(\Delta t)\,|00\rangle + \beta(\Delta t)\,|11\rangle$ by applying two pulses with time interval Δt in between to a two-level atom. This result is of great interest as it implies the possibility of removing the effect of the particular multi-photon error caused by the emission of two or more photons from the same photon source. For this reason a focus point for this thesis will be exploring the impact this multi-photon error has on the performance of certain protocols.

2 Quantum states and measurements

This thesis will be describing and carrying out calculations on many-particle systems. For this reason it will be useful to adopt the occupation-number representation of second quantization. This section will provide a brief overview of second quantization as well as the theoretical basis of quantum mechanical measurements.

2.1 Many-body systems in first quantization

A problem when describing quantum many-body systems is the principle of indistinguishability of identical particles. What this means is that opposed to classical mechanics where a particle can be equipped with an identifying marker, in quantum mechanics it is impossible to distinguish between identical particles. If a group of identical particles are then brought to the same region in space their wave functions will start to overlap making it impossible to tell which particle is where.

Let $\psi(r_1, r_2, ..., r_N)$ be the wave function describing a system of N particles. From the indistinguishability of particles follows that if two coordinates are interchanged the resulting state can at most differ by a prefactor λ. Change the same coordinates a second time and the resulting wave function must be exactly the same as the first:

$$\psi(r_1, ..., r_i, ..., r_j, ..., r_N) = \lambda\psi(r_1, ..., r_j, ..., r_i, ..., r_N) = \lambda^2\psi(r_1, ..., r_i, ..., r_j, ..., r_N) \tag{2.1}$$

From equation (2.1) we get $\lambda^2 = 1 \Rightarrow \lambda = \pm 1$. This leaves us with two distinct types of particles, namely bosons and fermions:

$$\psi(r_1, ..., r_i, ..., r_j, ..., r_N) = +\psi(r_1, ..., r_j, ..., r_i, ..., r_N) \qquad (Bosons) \tag{2.2}$$
$$\psi(r_1, ..., r_i, ..., r_j, ..., r_N) = -\psi(r_1, ..., r_j, ..., r_i, ..., r_N) \qquad (Fermions) \tag{2.3}$$

These are the symmetries that any multi-particle state must obey. This means the Hartree product of the single-particle basis states $\{\psi_{\nu(r)}\}$ which is given by $\Pi_{i=1}^{N}\psi_{\nu_i}(r_i)$ is not a valid basis because it is not properly symmetrized.

What we need are linear superpositions of products of the single-particle states. Take for instance the case where we have two particles in two different states. For the state of the two-particle system to obey the symmetry of bosonic particles in equation (2.2) it would need

to be:

$$|\Psi_B\rangle = \frac{1}{\sqrt{2}}(\psi_1(r_1)\psi_2(r_2) + \psi_1(r_2)\psi_2(r_1)) \tag{2.4}$$

And for the state to obey the symmetry of fermion particles in equation (2.3) it would need to be:

$$|\Psi_F\rangle = \frac{1}{\sqrt{2}}(\psi_1(r_1)\psi_2(r_2) - \psi_1(r_2)\psi_2(r_1)) \tag{2.5}$$

An example of three particle states for bosons and fermions can be found in appendix A.

For a general system of N particles the state can be constructed using a permanent for bosons and a Slater determinant for fermions.

$$\text{Permanent:} \quad \begin{vmatrix} \psi_{\nu_1}(r_1) & \psi_{\nu_1}(r_2) & \dots & \psi_{\nu_1}(r_N) \\ \psi_{\nu_2}(r_1) & \psi_{\nu_2}(r_2) & \dots & \psi_{\nu_2}(r_N) \\ \vdots & \vdots & \ddots & \vdots \\ \psi_{\nu_N}(r_1) & \psi_{\nu_N}(r_2) & \dots & \psi_{\nu_N}(r_N) \end{vmatrix}_+ = \sum_{p \in S_N} \left(\Pi_{i=1}^N \psi_{\nu_i}(r_{p(i)}) \right) \tag{2.6}$$

$$\text{Slater determinant:} \quad \begin{vmatrix} \psi_{\nu_1}(r_1) & \psi_{\nu_1}(r_2) & \dots & \psi_{\nu_1}(r_N) \\ \psi_{\nu_2}(r_1) & \psi_{\nu_2}(r_2) & \dots & \psi_{\nu_2}(r_N) \\ \vdots & \vdots & \ddots & \vdots \\ \psi_{\nu_N}(r_1) & \psi_{\nu_N}(r_2) & \dots & \psi_{\nu_N}(r_N) \end{vmatrix}_- = \sum_{p \in S_N} \left(\Pi_{i=1}^N \psi_{\nu_i}(r_{p(i)}) \right) sign(p) \tag{2.7}$$

With the sums being taken over all permutations p in the group of N! permutations denoted S_N and $sign(p)$ in the determinant is the sign of the permutation[3].

With the properly symmetrized and normalized states we have a basis for the Hilbert space of N particles. [2]

2.2 Second quantization

Building on the principles discussed in the previous chapter it is clear that only the occupied single-particle states are needed to describe the state of the many-body system. The occupation

[3] $sign(p) = 1$ for an even number of permutations and $sign(p) = -1$ for odd numbers of permutations

number representation of second quantization takes advantage of that. Instead of listing each particle and it's position, only the number of particles in each of the basis states is listed. Let n_{ν_i} be the occupation number of ψ_{ν_i}. This means an N-particle system would have the basis states:

$$|n_{\nu_1}, n_{\nu_2}, ..., n_{\nu_N}\rangle \tag{2.8}$$

with $\sum_{i=1}^{N} n_{\nu_i} = N$ and $n_{\nu_i} = \begin{cases} 0, 1, 2, ... & (Bosons) \\ 0, 1 & (Fermions) \end{cases}$

The restriction on fermions is due to the Pauli exclusion principle which states that a given quantum state in a quantum system cannot be occupied by more than one of the same type of fermion at any given point in time. This can be shown mathematically by considering equation (2.5). Suppose we have $\psi_1 = \psi_2$, then $|\Psi_F\rangle = 0$.

Definition 2.1. [Fock space] Let $\mathcal{F}$ refer to the space spanned by the basis states of the occupation number representation also called the Fock space. Let $\mathcal{F}_N$ be the space spanned by basis states in the occupation number representation with the same number of particles: $\mathcal{F}_N = span\{\, |n_{\nu_1}, n_{\nu_2}, ..., n_{\nu_N}\rangle \,|\, \sum_{i=1}^{N} n_{\nu_i} = N\}$

The Fock space $\mathcal{F}$ can then be defined as:

$$\mathcal{F} = \mathcal{F}_0 \otimes \mathcal{F}_1 \otimes \mathcal{F}_2 \otimes ... \tag{2.9}$$

With a set of basis states spanning the Fock space any quantum state in the Fock space can be constructed as a linear combination of the basis states.

We can define operators whose purpose is to raise or lower the number of particles in a given state. The operator who raises (lowers) the occupation number will be referred to as a creation (annihilation) operator and will be defined as follows: [2]

Definition 2.2. [Creation operator] Let $b^\dagger_{\nu_i}$ be an operator whose action on a state $\left|n_{\nu_1}, ..., n_{\nu_{i-1}}, n_{\nu_i}, n_{\nu_{i+1}}, ..., n_{\nu_N}\right\rangle$ will be defined as:

$$b^\dagger_{\nu_i} \left|n_{\nu_1}, ..., n_{\nu_{i-1}}, n_{\nu_i}, n_{\nu_{i+1}}, ..., n_{\nu_N}\right\rangle = \sqrt{n_{\nu_i} + 1} \left|n_{\nu_1}, ..., n_{\nu_{i-1}}, n_{\nu_i} + 1, n_{\nu_{i+1}}, ..., n_{\nu_N}\right\rangle \tag{2.10}$$

Definition 2.3. [Annihilation operator] Let b_{ν_i} be an operator whose action on a state $\left|n_{\nu_1}, ..., n_{\nu_{i-1}}, n_{\nu_i}, n_{\nu_{i+1}}, ..., n_{\nu_N}\right\rangle$ will be defined as:

$$b_{\nu_i} \left|n_{\nu_1}, ..., n_{\nu_{i-1}}, n_{\nu_i}, n_{\nu_{i+1}}, ..., n_{\nu_N}\right\rangle = \sqrt{n_{\nu_i}} \left|n_{\nu_1}, ..., n_{\nu_{i-1}}, n_{\nu_i} - 1, n_{\nu_{i+1}}, ..., n_{\nu_N}\right\rangle \tag{2.11}$$

2.3 Measurements

Having introduced the notation used for quantum states we will now move on to establish the framework of measurements.

For the purpose of this thesis we will adopt the definition of measurements posed in [3]. This means for a measurement on a system in state $|\psi\rangle$ with outcomes $\{m\}$ and corresponding measurement operators $\{M_m\}$ the probability to get outcome "m" will be given by Eq. (2.92) in [3]:

$$p_m = \langle\psi| M_m^\dagger M_m |\psi\rangle \tag{2.12}$$

And the state after measurement given outcome "m" is given by Eq. (2.93) in [3]:

$$|\psi\rangle_{after} = \frac{M_m |\psi\rangle_{initial}}{\sqrt{p_m}} \tag{2.13}$$

Since this thesis will not exclusively use the state vector representation but also the density matrix representation of quantum states, a definition of density matrices and their properties will be provided.

Suppose a quantum system has probabilities $\{p_i\}$ to be in a number of different quantum states[4] $\{|\psi_i\rangle\}$. The density matrix of such a quantum system will be defined as:

Definition 2.4. [Density matrix] Let a mixed quantum state be given by the ensemble: $\{p_i, |\psi_i\rangle\}$ with $i \in [1, N]$. We define the density matrix of that quantum state to be: [3]

$$\rho = \sum_{i=1}^{N} p_i |\psi_i\rangle \langle\psi_i| \tag{2.14}$$

The reason why this is a useful representation of a quantum state becomes clear once we describe measurements in this notation.

First consider the probability to get an outcome "m", assuming the system is in $|\psi_i\rangle$. From Eq. (2.12) this gives:

$$p(m|i) = \langle\psi_i| M_m^\dagger M_m |\psi_i\rangle = Tr(M_m^\dagger M_m |\psi_i\rangle \langle\psi_i|) \tag{2.15}$$

[4]This is referred to as a *mixed* quantum state or an *ensemble* of quantum states.

Given that "being in state i" is independent from the event "being in state j", the total probability to get an outcome "m" must be given by:

$$p_m = \sum_{i=1}^{N} p(m|i)p_i = \sum_{i=1}^{N} p_i Tr(M_m^\dagger M_m \left|\psi_i\right\rangle \left\langle\psi_i\right|) = Tr(M_m^\dagger M_m \rho) \tag{2.16}$$

From Eq. (2.13) we can get the state after measurement given the system was initially in state $|\psi_i\rangle$, and assuming an outcome "m":

$$\left|\psi_i^m\right\rangle = \frac{M_m \left|\psi_i\right\rangle}{\sqrt{p(m|i)}} \tag{2.17}$$

This means the resulting state becomes an ensemble of states $|\psi_i^m\rangle$ with each of the quantum states in the ensemble having the corresponding probability $p(i|m)$.

This means the resulting ensemble must be described by the density matrix:

$$\rho_m = \sum_{i=1}^{N} p(i|m) \left|\psi_i^m\right\rangle \left\langle\psi_i^m\right| = \sum_{i=1}^{N} p(i|m) \frac{M_m \left|\psi_i^m\right\rangle \left\langle\psi_i^m\right| M_m^\dagger}{p(m|i)} \tag{2.18}$$

Now from Bayes' theorem we have:

$$p(A|B) = \frac{p(B|A)p(A)}{p(B)} \tag{2.19}$$

$$\Rightarrow p(i|m) = \frac{p(m|i)p_i}{p_m} \tag{2.20}$$

Inserting this in Eq. (2.18) the density matrix of a quantum state after a measurement with outcome "m" is therefore given by:

$$\rho_m = \frac{M_m \rho M_m^\dagger}{p_m} \tag{2.21}$$

With these tools we can begin exploring quantum repeater protocols.

3 The problem of long-distance quantum communication

This section will motivate quantum repeaters in general as an alternative to direct transmission. In addition it will discus the problems quantum repeaters face when errors and imperfections are introduced and how these affect their performance. In doing so it will also introduce the focus of this thesis which is to study the effect of the multi-photon error terms in the source state.

3.1 Motivating repeaters

When sending light through fiber optic cables, there is an exponential loss related to the distance. The probability that a photon sent trough a fiber optic cable of length L will emerge at the other end is:

$$P = e^{-L/L_{att}} \tag{3.1}$$

L_{att} being the fiber attenuation length. In this thesis we will assume $L_{att} = 22$ km. This means for $L = 100$ km we get $P = 1.06\,\%$. This is quite low, but with enough photons it might still work. However, if $L = 1000$ km we get $P = 1.82 \cdot 10^{-20}\%$ which is too low to be able to work with.

The problem of loss was solved classically using amplification. Repeater nodes were placed at regular intervals, and at each node the signal was measured and then amplified before being sent to the next node, until the signal had finally reached the receiver.

In quantum mechanics the no-cloning theorem prevents copying of an unknown quantum state. This means amplification would not work for transmitting quantum information.

3.1.1 Proof of the no-cloning theorem

Suppose we have an arbitrary state $|\psi\rangle = a\,|0\rangle + b\,|1\rangle$ and want to clone it. Now let's assume we have a unitary operator U which can clone any arbitrary state such that:

$$U(|\psi\rangle\,|x\rangle) = |\psi\rangle\,|\psi\rangle \tag{3.2}$$

This must also be true for some other arbitrary state $|\phi\rangle$:

$$U(|\phi\rangle |x\rangle) = |\phi\rangle |\phi\rangle \tag{3.3}$$

Where $|x\rangle$ in both cases is some state to be changed into a clone.

For the proof let's consider:

$$\langle\psi|\phi\rangle \langle x|x\rangle = \langle\psi| \langle x| \ \ |\phi\rangle |x\rangle = \langle\psi| \langle x| U^\dagger U |\phi\rangle |x\rangle \tag{3.4}$$

Note in the last step it was used that U is unitary, so $U^\dagger U = \mathbb{1}$. Continuing we get:

$$\langle\psi| \langle x| U^\dagger U |\phi\rangle |x\rangle = \langle\psi| \langle\psi|\phi\rangle |\phi\rangle = \langle\psi|\phi\rangle \langle\psi|\phi\rangle = |\langle\psi|\phi\rangle|^2 \tag{3.5}$$

But this means we have: $\langle\psi|\phi\rangle \langle x|x\rangle = |\langle\psi|\phi\rangle|^2$. Assuming $|x\rangle$ is normalized, meaning $\langle x|x\rangle = 1$ we have: $|\langle\psi|\phi\rangle| = |\langle\psi|\phi\rangle|^2$. This can only be true if $\langle\psi|\phi\rangle = 0$ or $\langle\psi|\phi\rangle = 1$. This is not true in general, and so by proof by contradiction quantum mechanics does not allow for cloning of unknown states.

3.2 The challenges of quantum repeaters

Quantum repeaters work instead by taking advantage of quantum mechanical properties such as entanglement. The purpose of a quantum repeater protocol is to create entanglement between the sender and receiver.

While quantum repeaters work great in theory when not taking imperfections into account it is not a realistic model of how it would work in practise. To get an accurate sense of how efficient a quantum repeater would be compared to direct transmission in a more real setting imperfections must be included.

One potential imperfection from the photon source are multi-photon errors. Suppose an atomic ensemble is used to store information and as a photon source. Let $|00\rangle$ be the state where there are no excitations in the ensemble, and no photons are emitted and let $|11\rangle$ be the state where there is one excitation in the ensemble and one photon is emitted respectively. It is often preferable if the state we get from our source only consists of these two terms. This is because an extra photon emitted from an ensemble causes either an increase in the time-cost of the protocol or a decrease in the fidelity of the resulting state. [4]

Interestingly it has been shown that it is possible to create a photon-number entangled state [1]. The principle was using a two-level system with ground state $|g\rangle$ and excited state $|e\rangle$ and

a spontaneous emission lifetime T_1. A pulse excites the system to the excited state $|e\rangle$ and at a time $t > 0$ the two-mode atom-photon system can be described as:

$$\alpha(t)\,|e\rangle\,|0\rangle + \beta(t)\,|g\rangle\,|1\rangle \tag{3.6}$$

With $\alpha(t) = e^{-t/2T_1}$ and $\beta = \sqrt{1-\alpha(t)^2}$. Adjacent time bins early (e) and late (l) can be defined. After a long time $t >> T_1$ the photon mode can be expected to be in the single-photon state $|1\rangle$. This state can be expressed in the time-bin notation as:

$$|1\rangle = \alpha(T)\,|0\rangle_e\,|1\rangle_l + \beta(T)\,|1\rangle_e\,|0\rangle_l \tag{3.7}$$

Where T is the chosen threshold dividing the early and late time bins. An illustration of the division of time into early and late bins can be seen in figure 1a.

Choosing the threshold T to be exactly the half-life of the source $T_{1/2} = ln(2)T_1$ the single-photon state becomes exactly the Bell-state: $|\psi^+\rangle = \frac{1}{\sqrt{2}}\big(\,|01\rangle + |10\rangle\,\big)$.

If a second pulse is then applied at time Δt after the first one consider the two options:

- No photon was emitted in the early bin i.e. the state was $|0\rangle_e\,|1\rangle_l$. This would imply the atom is still in the excited state $|e\rangle$ and has not yet emitted a photon at Δt. By applying a second pulse the atom is flipped back to the ground state $|g\rangle$ preventing the emission of a photon at a later point.
- If a photon was emitted in the early bin i.e. the state was $|1\rangle_e\,|0\rangle_l$ the atom is in the ground state $|g\rangle$ at Δt. The application of the second pulse would then re-excite the atom causing the emission of another photon at a later point.

Consequently considering the state of the photon given by Eq. (3.7) at time $T = \Delta t$ the single-photon state becomes:

$$\alpha(\Delta t)\,|0\rangle_e\,|0\rangle_l + \beta(\Delta t)\,|1\rangle_e\,|1\rangle_l \tag{3.8}$$

An illustration of the effect of applying a second pulse on the single-photon state can be found in figure 1b.

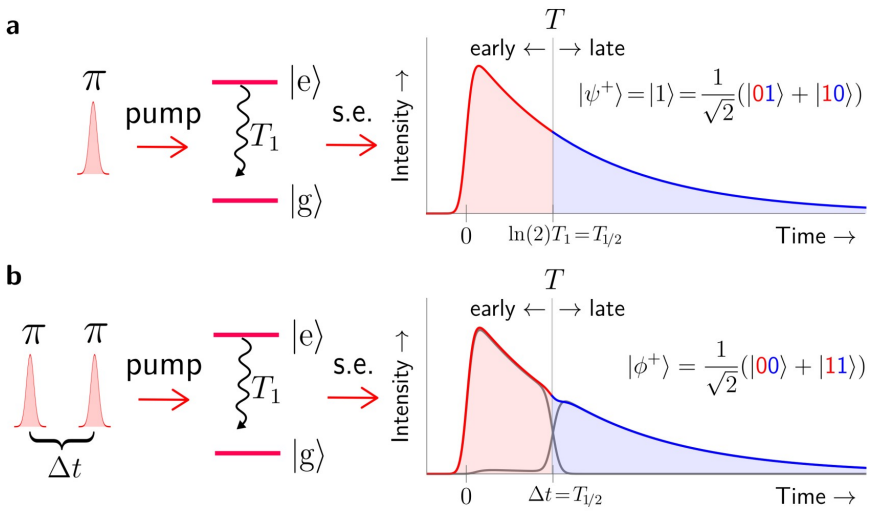

Figure 1: **Generation of photon number Bell-states:** a) The time is separated into two bins: early (e) and late (l). The single-photon state can then be described in the time-bin notation as the Bell-state $|\psi^+\rangle$. b) A second pulse is applied at the half-life $T_{1/2} = ln(2)T_1$. This causes the single-photon state to then be flipped to the Bell-state $|\phi^+\rangle$. [1]

This is the motivation for the focus of this thesis which will be to calculate how effective certain repeater protocols become if we can repress or even "turn off" the term $|22\rangle$.

4 Building blocks of quantum repeaters

This section will discuss similarities between repeater protocols. It will describe how atomic ensembles can be used as quantum memories and it will introduce how entanglement generation and swapping work mathematically by exploring a simple quantum repeater scheme, where the generation and swapping schemes are based on the detection of a single photon in a detector. For now ideal conditions will be assumed[5].

Repeater protocols can be constructed in a number of different ways, but in general a quantum repeater always has these elements: [4]

- A photon source
- Quantum memories.
- A process to generate entanglement.
- A process to do entanglement swapping.

They work by having a number of repeater nodes in between the sender and receiver. Entanglement is then created between the nodes. Once entanglement has been achieved between all the nodes, entanglement swapping is used to finally create entanglement between the sender and receiver node. It is important to note here the importance of being able to store entanglement. Since entanglement needs to be created between all nodes, should the entanglement generation fail between any of the nodes, the process has to be started all over again if the entanglement cannot be stored in the ones that were successful. An illustration of the process can be found in figure 2 below.

[5]This means no loss in the fibers, perfect detector efficiency and no dark counts or other imperfections. Imperfections will be introduced in a later section

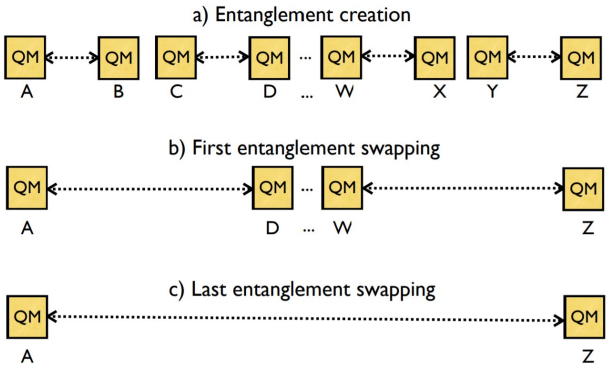

Figure 2: An illustration of the process behind a quantum repeater. The yellow squares represent quantum memories, and the dotted lines with arrows represent entanglement between links. a) First entanglement is created over the short distances between the links. b) Using entanglement swapping, links at further distances are now connected by entanglement. c) The last swap finally connects A and Z. [4]

The number of swappings needed to achieve entanglement over the full distance depends on the number of repeater nodes. This is called *the nesting level*. Let L_0 be the distance between the repeater nodes and L being the total distance between the sender and the receiver. L_0 is related to the nesting level by:

$$L_0 = \frac{L}{2^n} \tag{4.1}$$

4.1 Quantum memory and photon source

There are a number of ways to store quantum information and depending on what is studied they might be more or less useful. One of the simpler ways to store quantum information is choosing two states of a single atom to represent $|0\rangle$ and $|1\rangle$. In this way the atom can represent a qubit and in many cases this is a very useful and efficient way to do it. Single atoms and single photons couple very weakly though and in the repeater schemes which will be discussed in this thesis photons will be used as carriers of quantum information. The solution is to not use a single atom but to use an *ensemble* of atoms as quantum memories. This is more inefficient - more atoms are used to store the same amount of information. In some cases it makes sense however to get more interaction between the atoms and photons.

Suppose we have an ensemble with N atoms and they all start in the state $|0\rangle$. Let $s^\dagger$ be an operator that takes the state $|0, 0, ..., 0, 0\rangle$ into a symmetric superposition of states with one

atom excited:

$$s^\dagger |0,0,...,0,0\rangle = \frac{1}{N}\sum_{m=1}^{N} |0,...,0,1_m,0,...,0\rangle \tag{4.2}$$

$|0,...,0,1_m,0,...,0\rangle$ represents the state where only the m'th atom is excited and all others are in the state $|0\rangle$. These collective modes resemble the Fock states of a harmonic oscillator with annihilation operator s and creation operator $s^\dagger$:

$$|n\rangle = \frac{(s^\dagger)^n}{\sqrt{n!}} |0\rangle \tag{4.3}$$

It is in these states quantum information can be stored.

There are different processes to store and retrieve information from the ensembles. This thesis will not go into details about the storage and retrieval processes. It will however provide a brief example of how these procedures might be done.

The process described in [4] uses an ensemble of atoms with two stable ground states $|g_1\rangle$ and $|g_2\rangle$ and an excited state $|e\rangle$. All atoms in the ensemble will be assumed to initially be in $|g_1\rangle$.

The process for storing quantum information will also be referred to as the write process. To store quantum information a pulse is used to create collective excitations in the ensemble by spontaneous Raman emission. The emitted photon will be referred to as a Stokes photon.

The process for reading out the excitation in the ensemble also uses a pulse to excite the $g_2 - e$ transition which is then followed by the emission of a photon on the $e - g_1$ transition.

An illustration of the write- and read processes can be found in figure 3.

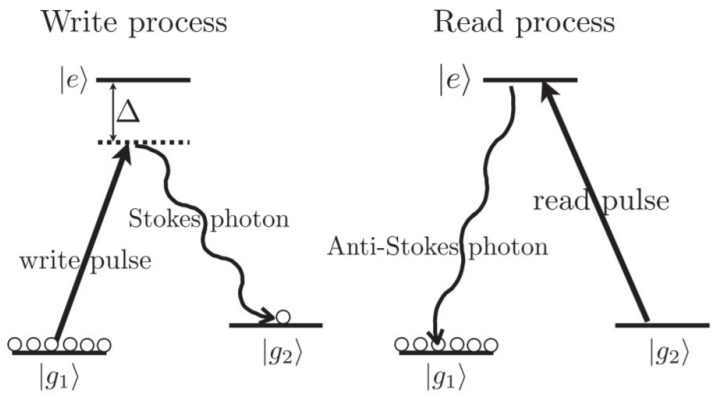

Figure 3: An illustration of the write process (left) and read process (right) used to store and retrieve quantum information from atomic ensembles. Write process: All atoms are assumed to initially be in the $|g_1\rangle$ state. A pulse off-resonantly drives the $g_1 - e$ transition followed by the emission of a photon on the $e - g_2$ transition. Read process: a pulse on the $g_2 - e$ transition is applied followed by the emission of a photon on the $e - g_1$ transition. [4]

From Eq. (5) in the paper [4] the write process is shown to create the two-mode entangled state:

$$\left(1 - \frac{1}{2}(\chi t)^2\right)|00\rangle - i\chi t\,|11\rangle - (\chi t)^2\,|22\rangle + \mathcal{O}((\chi t)^3) \tag{4.4}$$

Where the first mode is the state of the ensemble, i.e. the memory mode and the second mode is the photon mode.

Dividing all terms by $\left(1 - \frac{1}{2}(\chi t)^2\right)$ we get:

$$1 \cdot |00\rangle - \frac{i\chi t\,|11\rangle}{\left(1 - \frac{1}{2}(\chi t)^2\right)} - \frac{(\chi t)^2\,|22\rangle}{\left(1 - \frac{1}{2}(\chi t)^2\right)} \tag{4.5}$$

Using the Taylor-expansion of $\frac{1}{1-x} = \sum_{n=0}^{\infty} x^n$ and taking it to first order we get $-\frac{i\chi t\,|11\rangle}{\left(1 - \frac{1}{2}(\chi t)^2\right)} = -i\chi t \frac{1}{1 - \frac{1}{2}(\chi t)^2}\,|11\rangle \approx -i(\chi t)\,|11\rangle$. In the same way from the second term we get: $-\frac{(\chi t)^2\,|22\rangle}{\left(1 - \frac{1}{2}(\chi t)^2\right)} = -(\chi t)^2 \frac{1}{1 - \frac{1}{2}(\chi t)^2}\,|22\rangle \approx -(\chi t)^2\,|22\rangle$.

This means if we assume the ensemble emits a photon with some small probability $p = (\chi t)^2$,

the un-normalized source state is:

$$|\Psi\rangle = |00\rangle - i\sqrt{p}\,|11\rangle - p\,|22\rangle \tag{4.6}$$

Defining $|11\rangle$ as the result of some creation operator on $|00\rangle$: $s_a^\dagger a^\dagger\,|00\rangle$ we can include the phase $-i$ in the definition of the creation operator.

$$|\Psi\rangle = |00\rangle + \sqrt{p}\,|11\rangle + p\,|22\rangle \tag{4.7}$$

This source state introduces multi-photon errors in the shape of $|22\rangle$. Ideally the photon source would produce a source state $\sqrt{1-p}\,|00\rangle + \sqrt{p}\,|11\rangle$ which only has a probability to emit no photon or one photon.

Entanglement generation and entanglement swapping will be introduced assuming ideal conditions. For this reason the source state used will be assumed to be $\sqrt{1-p}\,|00\rangle + \sqrt{p}\,|11\rangle$. The source state from Eq. (4.7) will be used with the introduction of imperfections.

4.2 One-click entanglement generation

One of the ways in which entanglement can be generated between the two ensembles is through the detection of a single photon. Each ensemble can with some probability emit a photon which will travel through a beamsplitter and then hit one of two detectors. The setup is illustrated in figure 4.

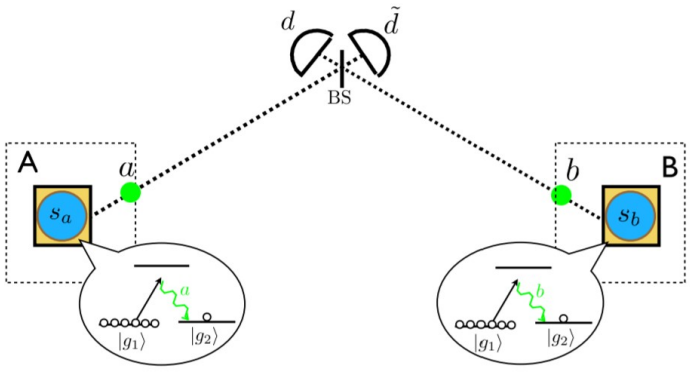

Figure 4: The setup of an entanglement generation process based on the detection of a single photon. A photon is emitted from either ensemble A or ensemble B and sent through a beamsplitter. The detection of a photon in either d or $\tilde{d}$ then creates entanglement between ensemble A and B. [4]

Let $s_a^\dagger$ ($s_b^\dagger$) be a bosonic operator that raises the excitation number in ensemble A (B) as described in Eq. (4.2). Let $|0\rangle_{m,A}$ be the state of the ensemble A where no atoms are excited and $|1\rangle_{m,A}$ be the state where a single atom is excited. [4]

Similarly let $a^\dagger$ ($b^\dagger$) be a bosonic creation operator that creates a photon coming from A (B).

Suppose a photon is emitted from the ensemble with some probability p. The state of ensemble A can then be described as:

$$|\Psi\rangle_A = \sqrt{1-p}\,|0\rangle_{m,A} \otimes |0\rangle_{ph,a} + \sqrt{p}\, s_a^\dagger a^\dagger\, |0\rangle_{m,A} \otimes |0\rangle_{ph,a} \tag{4.8}$$
$$= \sqrt{1-p}\,|0\rangle_{m,A} \otimes |0\rangle_{ph,a} + \sqrt{p}\,|1\rangle_{m,A} \otimes |1\rangle_{ph,a} \tag{4.9}$$

Here "m" and "ph" represent the memory modes and the photonic modes respectively in system A.

The state of system B will be completely equivalent. Letting $|AB\rangle$ denote the tensor product $|A\rangle \otimes |B\rangle$, the state of the combined system A and B then becomes:

$$|\Psi\rangle_{AB} = (1-p)\,|00\rangle_{m_A,m_B}\,|00\rangle_{ph_a,ph_b} + \sqrt{(1-p)p}\,(s_a^\dagger a^\dagger + s_b^\dagger b^\dagger)\,|00\rangle_{m_A,m_B}\,|00\rangle_{ph_a,ph_b} \tag{4.10}$$
$$+ p s_a^\dagger s_b^\dagger a^\dagger b^\dagger\,|00\rangle_{m_A,m_B}\,|00\rangle_{ph_a,ph_b}$$
$$= (1-p)\,|00\rangle_{m_A,m_B}\,|00\rangle_{ph_a,ph_b} + \sqrt{(1-p)p}\,(|10\rangle_{m_A,m_B}\,|10\rangle_{ph_a,ph_b} \tag{4.11}$$
$$+ |01\rangle_{m_A,m_B}\,|01\rangle_{ph_a,ph_b}) + p\,|11\rangle_{m_A,m_B}\,|11\rangle_{ph_a,ph_b}$$

The modes the photon can be detected in are: [4]

$$d_+ = \frac{1}{\sqrt{2}}(a+b), \qquad d_- = \frac{1}{\sqrt{2}}(a-b) \tag{4.12}$$

This means the measurement operators for one-click entanglement generation are given by:

$$M_+ = |\phi_+\rangle\langle\phi_+|, \qquad |\phi_+\rangle = d_+^\dagger\,|\varnothing\rangle = \frac{1}{\sqrt{2}}\big(\,|10\rangle + |01\rangle\,\big) \tag{4.13}$$
$$M_- = |\phi_-\rangle\langle\phi_-|, \qquad |\phi_-\rangle = d_-^\dagger\,|\varnothing\rangle = \frac{1}{\sqrt{2}}\big(\,|10\rangle - |01\rangle\,\big) \tag{4.14}$$

From Eq. (2.12) we can calculate the probability to get outcome d_+:

$$\langle\Psi|_{AB}\left(\mathbb{1}\otimes|\phi_+\rangle\langle\phi_+|\phi_+\rangle\langle\phi_+|\right)|\Psi\rangle_{AB} = \langle\Psi|_{AB}\left(\mathbb{1}\otimes|\phi_+\rangle\langle\phi_+|\right)|\Psi\rangle_{AB} \tag{4.15}$$

$$= \frac{(1-p)p}{2}(\langle 10|\langle 10| + \langle 01|\langle 01|)(\mathbb{1}\otimes|\phi_+\rangle\langle\phi_+|)(|10\rangle|10\rangle + |01\rangle|01\rangle) \tag{4.16}$$

$$= \frac{(1-p)p}{2}(\langle 10|10\rangle\langle 10|10\rangle + \langle 01|01\rangle\langle 01|01\rangle) = (1-p)p \tag{4.17}$$

Then from Eq. (2.13) we can calculate the state after measurement given outcome d_+:

$$|\Psi_0\rangle = \frac{(\mathbb{1}_{m_A,m_B}\otimes|\phi_+\rangle\langle\phi_+|_{ph_a,ph_b})|\Psi\rangle_{AB}}{\sqrt{\langle\Psi|\phi_+\rangle\langle\phi_+|\phi_+\rangle\langle\phi_+|\Psi\rangle}} \tag{4.18}$$

$$= \sqrt{\frac{(1-p)p}{(1-p)p\cdot 2}}\Big(|10\rangle_{m_A,m_B}|\phi_+\rangle\langle 10|10\rangle_{ph_a,ph_b} + |01\rangle_{m_A,m_B}|\phi_+\rangle\langle 01|01\rangle_{ph_a,ph_b}\Big) \tag{4.19}$$

$$= \frac{1}{\sqrt{2}}\Big(|10\rangle_{m_A,m_B}|\phi_+\rangle_{ph_a,ph_b} + |01\rangle_{m_A,m_B}|\phi_+\rangle_{ph_a,ph_b}\Big) \tag{4.20}$$

$$= \frac{1}{\sqrt{2}}\big(|10\rangle_{m_A,m_B} + |01\rangle_{m_A,m_B}\big)\otimes|\phi_+\rangle \tag{4.21}$$

In density matrix notation:

$$|\Psi_0\rangle\langle\Psi_0| = \frac{1}{2}(|10\rangle + |01\rangle)(\langle 10| + \langle 01|)\otimes|\phi_+\rangle\langle\phi_+| \tag{4.22}$$

$$= \frac{1}{2}(|10\rangle\langle 10| + |10\rangle\langle 01| + |01\rangle\langle 10| + |01\rangle\langle 01|)\otimes|\phi_+\rangle\langle\phi_+| \tag{4.23}$$

What we can see is that we end up with a completely separable state with the photon being in $|\phi_+\rangle$ and the two ensembles in a shared entangled state. Using the density matrix form of the state from equation 4.22 and tracing out the photon modes gives:

$$|\Psi\rangle\langle\Psi|_{m_A,m_B} = Tr_{ph}\big(|\Psi_0\rangle\langle\Psi_0|\big) \tag{4.24}$$

$$= \frac{1}{2}(|10\rangle\langle 10| + |10\rangle\langle 01| + |01\rangle\langle 10| + |01\rangle\langle 01|)\cdot trace\big(|\phi_+\rangle\langle\phi_+|\big) \tag{4.25}$$

$$= \frac{1}{2}(|10\rangle\langle 10| + |10\rangle\langle 01| + |01\rangle\langle 10| + |01\rangle\langle 01|) \tag{4.26}$$

$$\Rightarrow |\Psi\rangle_{m_A,m_B} = \frac{1}{\sqrt{2}}\big(|10\rangle + |01\rangle\big) \tag{4.27}$$

This is exactly the entangled state needed for the next step in the repeater protocol: entanglement swapping.

If the click was in d_- the calculations would be very similar except instead of $|\phi_+\rangle$ they would be carried out with $|\phi_-\rangle$ resulting in the final state being $|\Psi\rangle_{m_A,m_B} = \frac{1}{\sqrt{2}}\big(|10\rangle - |01\rangle\big)$. This does not change anything however considering a gate can be applied to change the state to be the same as the resulting state given a click in d_+ from Eq. (4.27). This means under ideal conditions it can be assumed that the entangled pairs will be in an entangled state like the one in Eq. (4.27) for the subsequent entanglement swapping steps. [4]

4.3 One-click entanglement swapping

Once entanglement has been established between the repeater nodes, entanglement swapping can be used to entangle nodes that are further apart. Repeating the swapping will then eventually lead to entanglement between the sender and receiver.

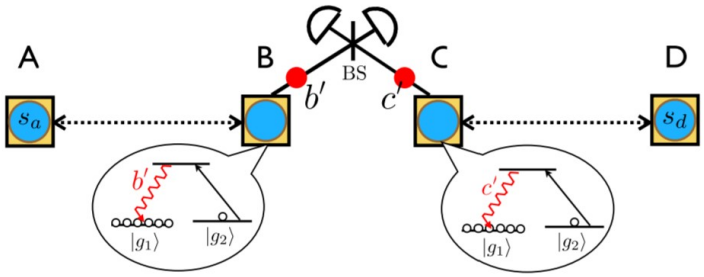

Figure 5: The setup of an entanglement swapping scheme based on the detection of a single photon. Entangled pairs of ensembles $A-B$ and $C-D$ are prepared and ensembles B and C are read out. If the ensembles have an excitation stored an anti-stokes photon will be emitted and then combined on a beamsplitter. The detection of a single photon in either of the two detectors then creates entanglement between ensembles A and D. [4]

Entanglement swapping can be achieved by measuring on ensembles B and C.

Suppose the ensembles A and B share the entangled state:

$$|\Psi\rangle_{AB} = \frac{1}{\sqrt{2}}\big(|10\rangle + |01\rangle\big) \tag{4.28}$$

Similarly, C and D share the entangled state:

$$|\Psi\rangle_{CD} = \frac{1}{\sqrt{2}}\big(|10\rangle + |01\rangle\big) \tag{4.29}$$

The combined shared state between nodes A, B, C and D is then:

$$|\Psi\rangle_{ABCD} = |\Psi\rangle_{AB} \otimes |\Psi\rangle_{CD} = \frac{1}{2}(|1010\rangle + |1001\rangle + |0110\rangle + |0101\rangle) \tag{4.30}$$

Now let ensembles B and C be read-out so an anti-stokes photon is emitted, if the ensemble is excited. Let $b'^{\dagger}$ denote the creation operator of an anti-Stokes photon coming from ensemble B.

The modes the photon can be detected in are: [4]

$$d_+ = \frac{1}{\sqrt{2}}(b + c), \qquad d_- = \frac{1}{\sqrt{2}}(b - c) \tag{4.31}$$

This means the measurement operators for one-click entanglement swapping are given by:

$$M_+ = |\phi_+\rangle \langle\phi_+|, \qquad |\phi_+\rangle = d_+^{\dagger} |\varnothing\rangle = \frac{1}{\sqrt{2}}\big(|10\rangle + |01\rangle \big) \tag{4.32}$$

$$M_- = |\phi_-\rangle \langle\phi_-|, \qquad |\phi_-\rangle = d_-^{\dagger} |\varnothing\rangle = \frac{1}{\sqrt{2}}\big(|10\rangle - |01\rangle \big) \tag{4.33}$$

Calculating the probability of getting for example outcome d_+ from Eq. (2.12) gives:

$$\langle\Psi|_{ABCD} (\mathbb{1} \otimes |\phi_+\rangle \langle\phi_+|\phi_+\rangle \langle\phi_+|) |\Psi\rangle_{ABCD} = \langle\Psi|_{ABCD} (\mathbb{1} \otimes |\phi_+\rangle \langle\phi_+|) |\Psi\rangle_{ABCD} \tag{4.34}$$

$$= \frac{1}{8}(\langle 1| \langle 01| \langle 0| + \langle 0| \langle 10| \langle 1|)(\mathbb{1} \otimes |\phi_+\rangle \langle\phi_+| \otimes \mathbb{1})(|1\rangle |01\rangle |0\rangle + |0\rangle |10\rangle |1\rangle) \tag{4.35}$$

$$= \frac{1}{8}(\langle 1|1\rangle \langle 01|01\rangle \langle 0|0\rangle + \langle 0|0\rangle \langle 10|10\rangle \langle 1|1\rangle) = \frac{1}{4} \tag{4.36}$$

And the state after measurement given outcome d_+ from Eq. (2.13):

$$|\Psi_1\rangle = \frac{(\mathbb{1}_{AD} \otimes |\phi_+\rangle \langle\phi_+|) |\Psi\rangle_{ABCD}}{\sqrt{\langle\Psi|\phi_+\rangle \langle\phi_+|\phi_+\rangle \langle\phi_+|\Psi\rangle}} \tag{4.37}$$

$$= \frac{1}{\sqrt{\frac{1}{4} \cdot 2 \cdot \sqrt{2}}}\Big(|1\rangle |\phi_+\rangle \langle 01|01\rangle |0\rangle |0\rangle |\phi_+\rangle \langle 10|10\rangle |1\rangle \Big) \tag{4.38}$$

$$= \frac{1}{\sqrt{2}}\Big(|1\rangle_A |\phi_+\rangle_{BC} |0\rangle_D + |0\rangle_A |\phi_+\rangle_{BC} |1\rangle_D \Big) \tag{4.39}$$

$$= \frac{1}{\sqrt{2}}\big(|10\rangle_{AD} + |01\rangle_{AD} \big) \otimes |\phi_+\rangle \tag{4.40}$$

Again the resulting state between A and D is a shared entangled state completely separable from the state of B and C.

Once entanglement has been established between A and D, one could imagine a similar pair of entangled ensembles E and H. Swapping again will then entangle ensembles A and H. This process can be continued an arbitrary number of times to entangle the sender and receiver nodes over an arbitrarily long distance. [4]

4.4 Performance

To compare the performance of different quantum repeater protocols under varying conditions two important values were calculated; the fidelity of the final state and the total time the protocol needs to run.

4.4.1 Fidelity and post-selection

Fidelity is a measure of how similar two quantum states are. It is the probability of being able to distinguish the two by some quantum measurement.

We will define the fidelity as:

Definition 4.1. [**Fidelity**] Let ρ and σ be the density operators of two quantum states. The fidelity $F(\rho, \sigma)$ will be given as:

$$F(\rho,\sigma) = \left(Tr\left(\sqrt{\sqrt{\sigma}\rho\sqrt{\sigma}}\right)\right)^2 \tag{4.41}$$

Suppose one of the two density matrices is pure i.e. it can be represented as the outer product of a state vector with itself: $\sigma = |\Psi_\sigma\rangle\langle\Psi_\sigma|$. The expression for the fidelity then reduces to:

$$F(\rho,\sigma) = \left(Tr\left(\sqrt{\sqrt{\sigma}\rho\sqrt{\sigma}}\right)\right)^2 = \left(Tr\left(\sqrt{|\Psi_\sigma\rangle\langle\Psi_\sigma|\,\rho\,|\Psi_\sigma\rangle\langle\Psi_\sigma|}\right)\right)^2 \tag{4.42}$$

$$= \langle\Psi_\sigma|\,\rho\,|\Psi_\sigma\rangle \left(Tr\left(\sqrt{|\Psi_\sigma\rangle\langle\Psi_\sigma|}\right)\right)^2 = \langle\Psi_\sigma|\,\rho\,|\Psi_\sigma\rangle \tag{4.43}$$

If both states are pure i.e. $\rho = |\Psi_\rho\rangle\langle\Psi_\rho|$ and $\sigma = |\Psi_\sigma\rangle\langle\Psi_\sigma|$ it follows from Eq. (4.43) that the expression for the fidelity reduces further:

$$F(\rho,\sigma) = \langle\Psi_\sigma|\,\rho\,|\Psi_\sigma\rangle = \langle\Psi_\sigma|\Psi_\rho\rangle\langle\Psi_\rho|\Psi_\sigma\rangle = |\langle\Psi_\rho|\Psi_\sigma\rangle|^2 \tag{4.44}$$

If $\rho = \sigma$ from the definition 4.1 of the fidelity:

$$F(\rho, \rho) = \left(Tr\left(\sqrt{\sqrt{\rho}\rho\sqrt{\rho}}\right)\right)^2 = \left(Tr(\rho)\right)^2 = 1 \tag{4.45}$$

Consider a protocol under ideal conditions using the one-click entanglement generation and the one-click swapping schemes discussed in chapters 4.2 and 4.3 to distribute entanglement across some distance. As calculated in Eq. (4.40) the final state between ensembles A and Z can be guaranteed to be in the entangled state $|\Psi\rangle_{AZ} = \frac{1}{\sqrt{2}}\left(|10\rangle_{AZ} + |01\rangle_{AZ}\right)$. The density matrix must thereby be given as: $\rho_{AZ} = |\Psi\rangle\langle\Psi|_{AZ}$. This is exactly the desired entangled state and so the fidelity between the actual final state and the desired state can therefore be found to be:

$$F(\rho_{AZ}, \rho_{AZ}) = 1 \tag{4.46}$$

This is not surprising as no imperfections have been introduced to cause a decrease in fidelity.

Suppose somehow the fidelity of the final state was *not* 1. This is where post-selection becomes a useful tool.

Post-selection is a method to increase the fidelity of the final state. It works by reading out the excitations stored in the ensembles after the quantum repeater protocol has been run. In this way the probability of detecting and rejecting unwanted states become higher.

Suppose entanglement has been established between two pairs of ensembles across the desired distance between the sender at position A and the receiver at position Z. This means there are two entangled pairs $A_1 - Z_1$ and $A_2 - Z_2$. An illustration of the post-selection scheme setup can be found in figure 6.

The excitations stored at each location are read out and the emitted anti-stokes photons are then sent through beamsplitters. If and only if one photon is detected at each location A and Z is the post-selection process accepted.

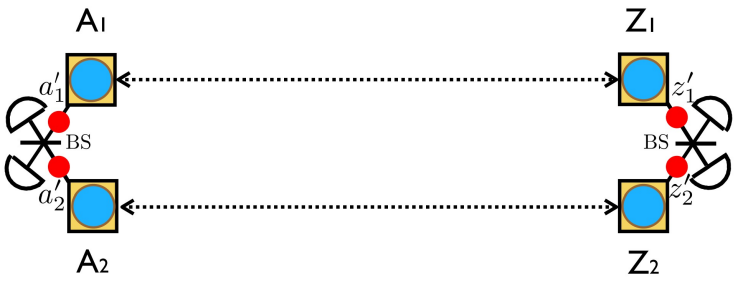

Figure 6: Setup of the post-selection scheme. Two pairs of entangled ensembles are prepared and at each location A and Z the excitations in the ensembles are read out and the emitted anti-stokes photons are sent through a beamsplitter.

This means suppose there is vacuum at A_1 and Z_1 i.e. no excitations to be read out. This would mean assuming nothing else went wrong only there would have to be excitations in both A_2 and Z_2 for the post-selection to be successful. Of course imperfections might also influence the post-selection, but it goes to show the probability of catching unwanted states increases thereby improving the fidelity.

Of course adding a post-selection step may increase the fidelity but at the cost of time. If only one-click generation and one-click swapping were used entanglement needs to be prepared between both pairs of ensembles. In other words two independent events need to occur which takes time. Furthermore there is a chance the post-selection is un-successful and the entire repeater protocol needs to be started over.

4.4.2 Total time

While the fidelity is an important aspect of a repeater protocol, for it to be useful it also needs to have a reasonable time scale. This means we need a formula to calculate the total time cost of a repeater protocol. That is we need a formula to calculate the combined time for each step in the protocol to be accepted including the final post-selection step.

Let $\{P_0, P_1, ..., P_n\}$ be the probabilities that a step in the repeater protocol is accepted. P_0 would for example be the probability to accept a click in the entanglement generation process. Likewise P_1 would be the probability to accept the first swap and so on. $\frac{L_0}{c}$ is the time it takes for a signal to travel between the elementary links with $L_0 = \frac{L}{2^n}$. Finally let $\{f_0, f_1, ..., f_{n-1}\}$ be the added factors when taking into account that not just one but two independent events need to occur[6]. In other words we need to wait for the preparation of two pairs of entangled ensembles when using the one-click entanglement swapping scheme. The total time without post-selection is then given by: [4]

$$T_{tot} = \frac{L_0}{c}\frac{f_0 f_1 ... f_{n-1}}{P_0 P_1 ... P_n} \tag{4.47}$$

As calculated in Eq. (4.46) under ideal conditions post-selection is not really necessary as the final state already has a fidelity of 1. When including imperfections however post-selection begins to be very useful in increasing the fidelity of the final state. Let P_{ps} be the probability for the post-selection process to be accepted. Additionally another factor of f is needed since the post-selection step requires another two pairs of entangled ensembles to be prepared. The

[6]The value of f was given in [4] to be $\frac{3}{2}$ when two independent events need to occur. Note however that for protocols using the two-click swapping methods, the first swap will need *four* independent events to occur. In this case $f = \frac{25}{12}$

total time when including post-selection thereby becomes: [4]

$$T_{tot} = \frac{L_0}{c} \frac{f_0 f_1 ... f_n}{P_0 P_1 ... P_n P_{ps}} \tag{4.48}$$

As an example consider the protocol under ideal conditions mentioned previously which uses the one-click entanglement generation and one-click entanglement swapping schemes.

Suppose $L = 1000$ km and 3 swaps are performed which means $L_0 = 125$ km. From Eq. (4.17) the probability of getting a click in d_+ in the entanglement generation step under ideal conditions is $(1-p)p$. Note the process is also accepted given a click in d_- which has the same probability. The overall probability to accept the entanglement generation step is thereby $P_0 = 2p(1-p)$.

For the entanglement swapping step it was calculated in Eq. (4.36) that the probability to get a click in d_+ given that the ensembles A, B, C and D are in the entangled state in Eq. (4.30) was $\frac{1}{4}$. As argued it is a fair assumption that A, B, C and D share that particular entangled state as the protocol can be constructed thereafter. Completely equivalently the swapping process is accepted given a click in d_- which happens with a probability of $\frac{1}{4}$ as well. This means the total probability of success for the swapping steps under ideal conditions is $P_1 = P_2 = P_3 = \frac{1}{2}$.

Given ideal assumptions are assumed post-selection would not be beneficial and so the total time can be calculated using Eq. (4.47):

$$T_{tot} = \frac{125 \ km}{2 \cdot 10^5 \ km/s} \cdot \frac{\left(\frac{3}{2}\right)^2}{2p(1-p) \cdot \left(\frac{1}{2}\right)^3} = \frac{5.62 \cdot 10^{-3}}{p(1-p)} \ s \tag{4.49}$$

The maximum value of $p(1-p)$ is at $p = 0.5$. The lowest possible time must be at this value of p meaning $T_{optimal} = 2.25 \cdot 10^{-2} \ s$.

This is fast distribution of quantum entanglement. Recall the probability of a photon reaching the receiver by direct transmission for $L = 1000$ km was $1.93 \cdot 10^{-20}\%$. Of course we have yet to take imperfections into account and this is where quantum repeater protocols begin to be less efficient.

5 Imperfections

It has now been shown that repeater protocols work in theory under ideal assumptions. This is not a realistic representation of how a quantum repeater would work in practise however.

To have the theoretical description of the quantum repeater protocols resemble reality more closely, we will in this section begin to describe various imperfections and how to include them when calculating the efficiency of a repeater protocol.

This section will discuss the various imperfections that might affect the repeater protocols discussed in this thesis and how they were taken into account in calculations.

5.1 Multi-photon errors

An important imperfection to take into account is the fact that an atomic ensemble has the probability to emit more than one photon. The ideal state from Eq. (4.8) is no longer a good representation seeing as $|00\rangle$ and $|11\rangle$ are no longer the only states the source can be found in. A better representation of the source state is seen in Eq. (4.7)

When allowing for the possibility of the emission of two or more photons it results in a nonzero chance of the detection of two photons. Assuming the detectors are number-resolving and no other imperfections, this will not cause an accept of an unwanted state in itself. It does increase the time cost as the process is restarted.

Another important consequence when allowing for the emission of multiple photons is in combination with other imperfections: photon loss and detector efficiency. Suppose two photons are emitted but one of them is either lost to the environment in the fiber optic cables or simply not detected. This causes an accept of an unwanted state. This means not only does the inclusion of imperfections slow down repeater protocols, they also give a non-zero chance to end up with a wrong state i.e. they decrease the fidelity of the final state.

5.2 Photon loss

Photon loss is the cause of the problem of long-distance quantum communication as discussed in a previous section. Even though the loss is much less for smaller distances, it is not removed entirely. The swapping schemes are local operations and so photon loss does not play a significant role. In the entanglement generation scheme however the distance between ensemble A and B is L_0. This means the distance between the ensembles and the detectors is $L_0/2$. The

transmission efficiency must thereby be given as:

$$\eta_t = exp\Big(\frac{-L_0}{2 \cdot 22}\Big) = e^{-L_0/44} \tag{5.1}$$

To include photon loss in calculations consider the state in equation (4.7). It had memory modes and photonic modes. If we include the environment we can add a term where the photon does not appear in the photon modes, but in the environment. In other words the photon is lost to the environment. The state of A can then be split up in an ideal part[7] and a part that contains the terms that accounts for photon loss. Let η_t be the probability that a photon is transmitted through the cable. In other words it is the probability given in equation (3.1). The un-normalized source state is then given by:

$$\begin{aligned}
|\Psi\rangle &= |\psi\rangle_{ideal} + |\psi\rangle_{loss} && (5.2)\\
\Rightarrow |\psi\rangle_{ideal} &= |\psi\rangle_{m,ph,ideal} \otimes |0\rangle_e && (5.3)\\
&= (|00\rangle_{m,ph} + \sqrt{p \cdot \eta_t}\,|11\rangle_{m,ph} + p \cdot \eta_t\,|22\rangle_{m,ph}) \otimes |0\rangle_e && (5.4)\\
\Rightarrow |\psi\rangle_{loss} &= \sqrt{p(1-\eta_t)}\,|10\rangle_{m,ph} \otimes |1\rangle_e && (5.5)\\
&+ p\sqrt{\eta_t(1-\eta_t)}\,|21\rangle_{m,ph} \otimes |1'\rangle_e + p(1-\eta_t)\,|20\rangle_{m,ph} \otimes |2\rangle_e && (5.6)
\end{aligned}$$

Now consider the density matrix of the state in Eq. (5.2):

$$\rho = |\Psi\rangle\langle\Psi| = |\psi\rangle_{ideal}\langle\psi|_{ideal} + |\psi\rangle_{ideal}\langle\psi|_{loss} + |\psi\rangle_{loss}\langle\psi|_{ideal} + |\psi\rangle_{loss}\langle\psi|_{loss} \tag{5.7}$$

Since we can't control the environment during experiments we will need to trace out the environment before doing measurements on the quantum state. Consider a term such as $|\psi\rangle_{ideal}\langle\psi|_{ideal}$:

$$\begin{aligned}
Tr_e\big(|\psi\rangle_{ideal}\langle\psi|_{ideal}\big) &= Tr_e\big(|\psi\rangle\langle\psi|_{m,ph,ideal} \otimes |0\rangle\langle 0|_e\big) && (5.8)\\
&= |\psi\rangle\langle\psi|_{m,ph,ideal} \cdot Tr(|0\rangle\langle 0|_e) = |\psi\rangle\langle\psi|_{m,ph,ideal} && (5.9)
\end{aligned}$$

And consider another term $|\psi\rangle_{ideal}\langle\psi|_{loss}$:

$$\begin{aligned}
Tr_e\big(|\psi\rangle_{ideal}\langle\psi|_{loss}\big) &= Tr_e\big(\sqrt{p(1-\eta_t)}\,|\psi\rangle_{m,ph,ideal}\langle 10|_{m,ph} \otimes |0\rangle\langle 1|_e && (5.10)\\
&+ p\sqrt{\eta_t(1-\eta_t)}\,|\psi\rangle_{m,ph,ideal}\langle 21|_{m,ph} \otimes |0\rangle\langle 1'|_e)\\
&+ p(1-\eta_t)\,|\psi\rangle_{m,ph,ideal}\langle 20|_{m,ph} \otimes |0\rangle\langle 2|_e\big) = 0
\end{aligned}$$

[7]Ideal here is a bit misleading. It is ideal with respect to photon loss in that no photons are lost, but since we include multi-photon emission terms it is not entirely ideal.

In all of these terms in the environment modes the 'ket' state is different from the 'bra' state in contrast to Eq. (5.8) where the environment modes were all the same i.e. $|0\rangle$. Therefore we have that $|\psi\rangle_{ideal}\langle\psi|_{loss}$ and $|\psi\rangle_{loss}\langle\psi|_{ideal}$ do not give contributions in a measurement since they are traced out.

Now consider $|\psi\rangle_{loss}\langle\psi|_{loss}$ and what happens when we take trace over the environment. The only terms where the 'ket' and 'bra' states of the environmental modes are the same must be: $p(1-\eta_t)|10\rangle\langle 10|_{m,ph}\otimes|1\rangle\langle 1|_e$, $p^2\eta_t(1-\eta_t)|21\rangle\langle 21|_{m,ph}\otimes|1'\rangle\langle 1'|_e$ and $p^2(1-\eta_t)^2|20\rangle\langle 20|_{m,ph}\otimes|2\rangle\langle 2|_e$

From this we can conclude that the only terms from the source state which give a non-zero contribution with photon loss and multi-photon emission terms taken into account must be:

$$\begin{aligned}\rho_{source} = |\psi\rangle\langle\psi|_{ideal} &+ p(1-\eta_t)|10\rangle\langle 10|_{m,ph} \\ &+ p^2\eta_t(1-\eta_t)|21\rangle\langle 21|_{m,ph} + p^2(1-\eta_t)^2|20\rangle\langle 20|_{m,ph}\end{aligned} \tag{5.11}$$

5.3 Efficiencies and dark counts

Detectors, as with much other equipment in physics in general, is unfortunately not perfect.

Two things can happen with detectors that need to be taken into account. First, even when a photon reaches the detector, there is a chance it might not register. The probability that a photon which has reached the detector will be registered will be referred to as the detector efficiency and will be denoted η_{det} in calculations. Second, even if there is no photon in the detector to trigger, it might still register a count. These are called dark counts and the probability to get a dark count in a detector will be denoted p_{dark} in calculations.

In addition to the imperfections related to the detectors there are inefficiencies relating to the atomic ensembles. The read-write processes described earlier are not infallible. With a certain probability η_{write} the ensemble will fail to store the excitation. Likewise with a probability η_{read} when performing the entanglement swapping there is a probability that the excitation will not be read out.

For the purpose of this thesis it will be assumed $\eta_{write} = 1$, however the effect of η_{read} will be explored in more detail.

6 First look at the effect of multi-photon errors

Since the main goal of this project is to explore the effect of the multi-photon errors in the source state it might be interesting to begin by looking at the extreme case where it is disregarded completely but other imperfections are included.

The case where the multi-photon error is disregarded will be referred to as having $dim = 2$ as the memory modes of the ensembles can only be in a state of no atoms being excited or one atom being excited. Likewise the photonic modes can only be occupied by no photons or one photon. This means the basis vectors of the modes are 2-dimensional:

$$|0\rangle = \begin{pmatrix} 1 \\ 0 \end{pmatrix}, \quad |1\rangle = \begin{pmatrix} 0 \\ 1 \end{pmatrix}$$

In the same way the case where it is accounted for in full will be referred to as $dim = 3$ seeing as now there is the possibility of two atoms being excited in the ensemble and to photons being emitted. This means the basis vectors are now 3-dimensional:

$$|0\rangle = \begin{pmatrix} 1 \\ 0 \\ 0 \end{pmatrix}, \quad |1\rangle = \begin{pmatrix} 0 \\ 1 \\ 0 \end{pmatrix}, \quad |2\rangle = \begin{pmatrix} 0 \\ 0 \\ 1 \end{pmatrix}$$

Simulating the standard Jiang protocol discussed in chapter 9 and plotting the fidelity as a function of p for $n = 3$ and for fixed parameters $L = 1000$ km, $\eta_{det} = \eta_{read} = 0.9$, $p_{dark} = 0$ and comparing $dim = 2$ with $dim = 3$ resulted in the plots found in figure 7

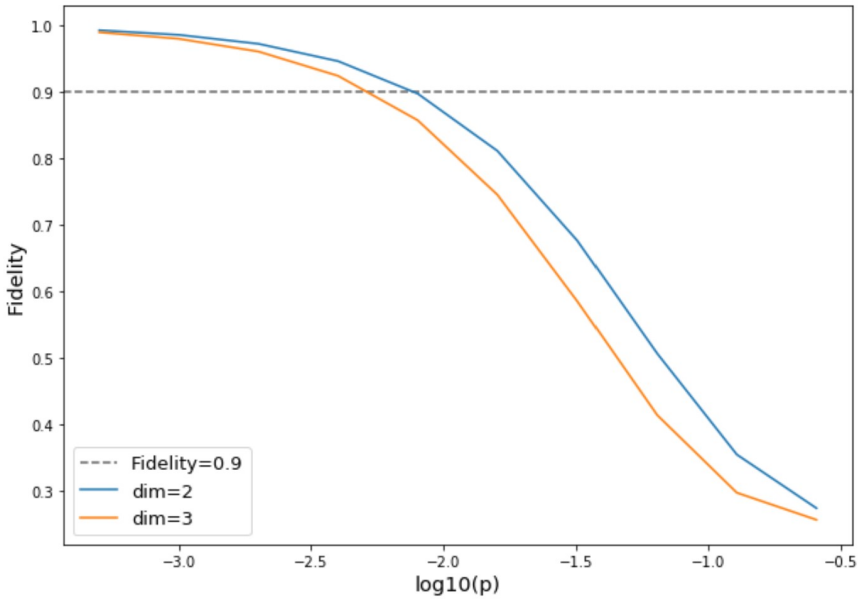

Figure 7: A plot of fidelity as a function of p. It compares $dim = 2$ with $dim = 3$ for the standard Jiang protocol. The other parameters were fixed at $L = 1000$ km, $n = 3$, $\eta_{det} = \eta_{read} = 0.9$ and $p_{dark} = 0$.

Similarly plotting time as a function of p for the same protocol and the same parameters produced the results found in figure 8.

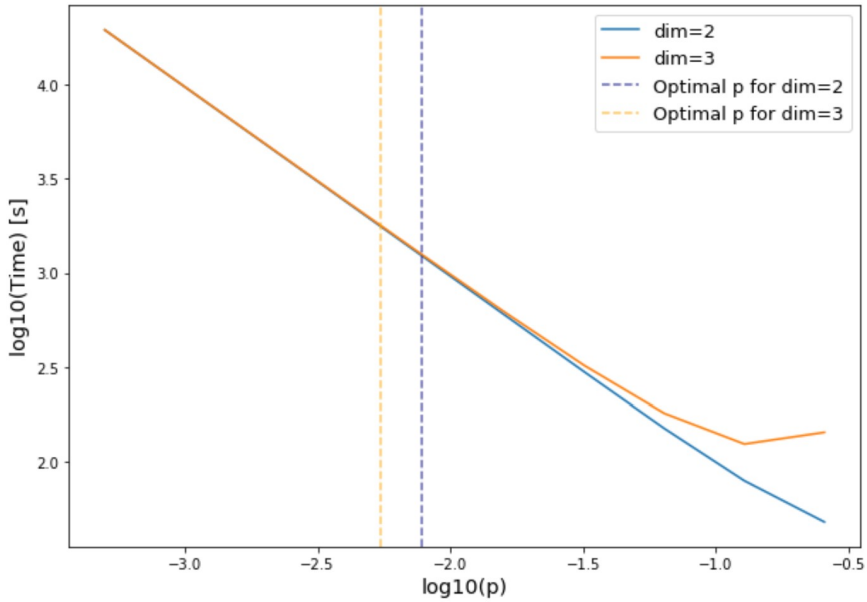

Figure 8: A plot of time as a function of p. It compares $dim = 2$ with $dim = 3$ for the standard Jiang protocol. The other parameters were fixed at $L = 1000$ km, $n = 3$, $\eta_{det} = \eta_{read} = 0.9$ and $p_{dark} = 0$.

Interestingly from figures 7 and 8 the time does not differ between $dim = 2$ and $dim = 3$ for values of p where the fidelity is somewhat acceptable. The fidelity is significantly better for $dim = 2$ however, which is to be expected when neglecting multi-photon errors.

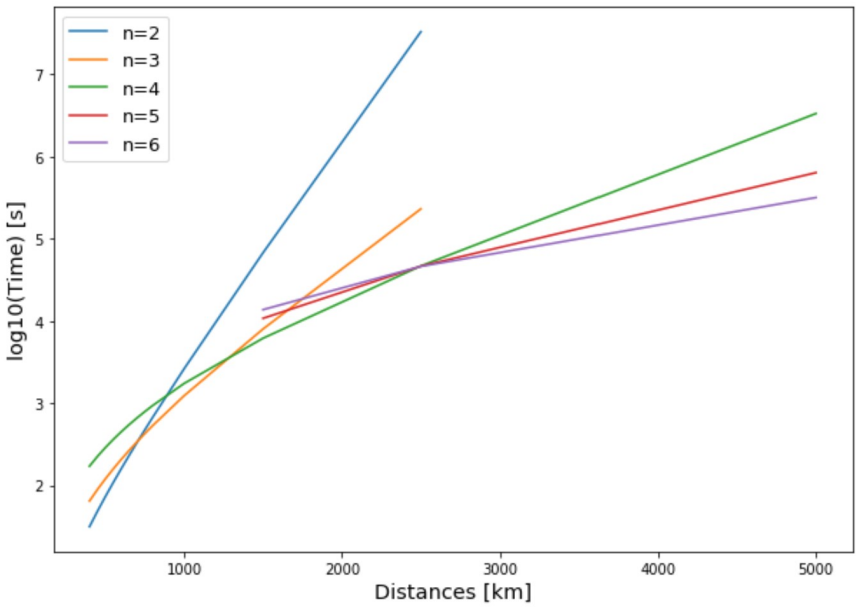

Figure 9: A plot of the optimal time as a function of distance for $n = 2$, $n = 3$ and $n = 4$ for $dim = 2$.

6.1 Newton-Raphson

Since for the most part the time seemed to go down as the value of p was increased[8] we can assume the best value of time can be found at the value of p where the fidelity is exactly at some minimum tolerated fidelity. For this project the minimum fidelity that was accepted was chosen to be 0.9.

To find the value of p in the point where the fidelity was 0.9 the Newton-Raphson root-finding algorithm was used.

Take a real-valued and differentiable function f with a root at x^*. The Newton-Raphson algorithm approximates the value x^* by taking an initial guess x_0 close to x^* and then finding a better guess by finding the root of the linear approximation in the point. This means the improved guess x_1 is found by:

$$f'(x_0) = \frac{f(x) - 0}{x_0 - x_1} \Rightarrow x_1 = x_0 - \frac{f(x_0)}{f'(x_0)} \tag{6.1}$$

In general if the algorithm is run n times then the n'th approximation is found by:

$$x_n = x_{n-1} - \frac{f(x_{n-1})}{f'(x_{n-1})} \tag{6.2}$$

There are issues related to this algorithm. The function must fulfill certain requirements and the initial guess must be chosen in a way that the algorithm actually converges toward the value of x^*.[9] If the initial value is chosen sufficiently close to x^* and the function satisfies the requirements it should find the root given enough time.

[8] At a high enough value of p the time did start to increase, but at this point the fidelity was so low that it was not in consideration regardless.

[9] Examples of what could go wrong include the algorithm getting stuck in a loop or finding the wrong root.

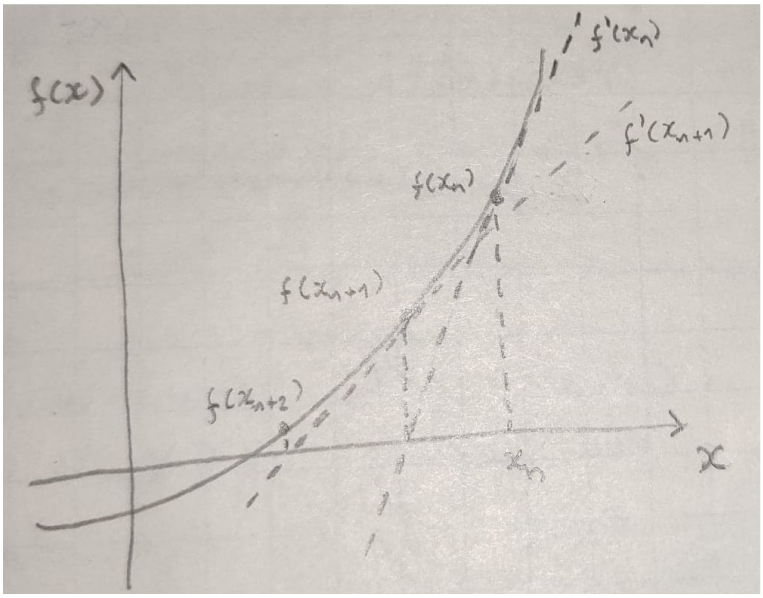

Figure 10: Illustration of the Newton-Raphson root finding algorithm. Once the approximation x_n has been found it is used as the input to find an improved approximation of the root value.

A concern might arise when finding the optimal value of p in this way. Given good enough conditions could it be that the optimal value of time was not found at the same value of p for which the fidelity was 0.9? Maybe a better time is found at a value of p where the fidelity is greater?

To explore this a simulation was run of the modified Jiang protocol with $\eta_{det} = 0.98$ and $\eta_{read} = 0.98$ and fixed parameters $L = 1000$ km, $p_{dark} = 0$ and $dim = 2$.

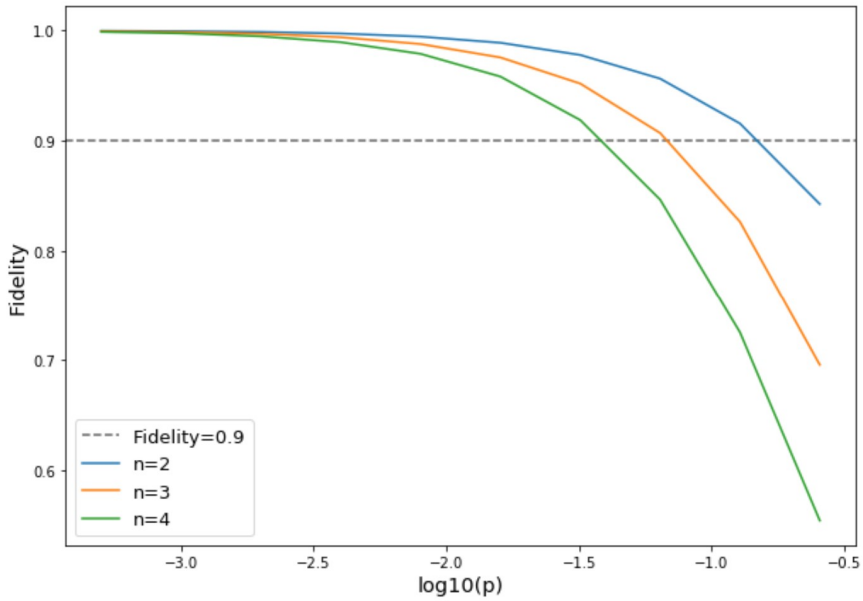

Figure 11: A plot of fidelity as a function of p for the modified Jiang protocol. Parameters $L = 1000$ km, $\eta_{det} = 0.98$ and $\eta_{read} = 0.98$, $p_{dark} = 0$ and $dim = 2$ were set to make conditions close to ideal. The dotted lines represent the value of p for which the fidelity was 0.9 for a given n.

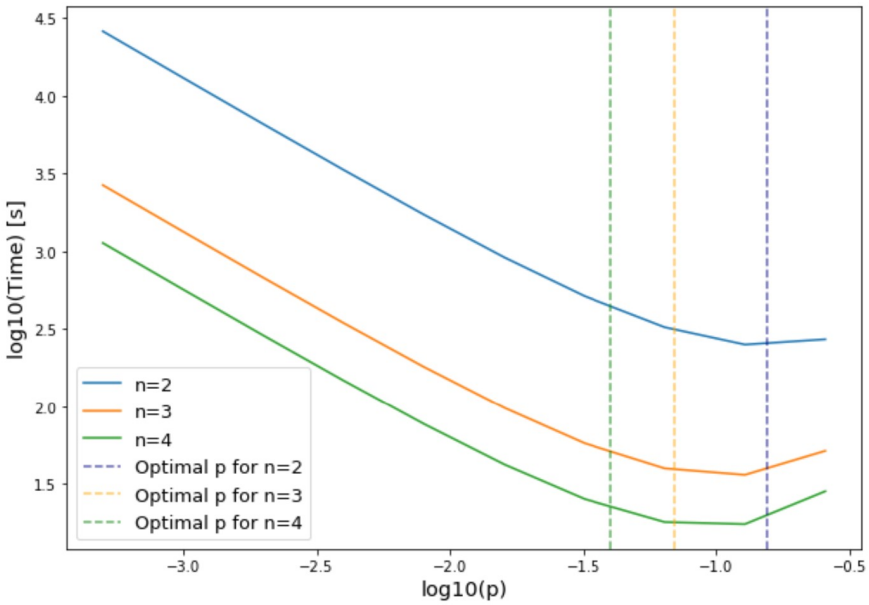

Figure 12: A plot of time as a function of p for the modified Jiang protocol. Parameters $L = 1000$ km, $\eta_{det} = 0.98$ and $\eta_{read} = 0.98$, $p_{dark} = 0$ and $dim = 2$ were set to make conditions close to ideal. The dotted lines represent the value of p for which the fidelity was 0.9 for a given n.

Evidently from the figures 11 and 12 when using as high efficiency as 0.98 problems do start to arise and one needs to be careful simply choosing the p for which the fidelity is 0.9 as the optimal p when operating in this regime. Consider the vertical dashed blue line representing

the value of p for which the fidelity was 0.9 for $n = 2$. It seems a slightly better time would be found by choosing a lower value of p resulting in a fidelity greater than 0.9. For $n = 3$ and $n = 4$ the value of p for which the fidelity was 0.9 does seem to find the lowest time.

That said an efficiency of 0.98 is far from a realistic representation of actual experimental equipment. Therefore so long as the efficiencies used in simulations are kept at more reasonable values the Newton-Raphson method should be effective at finding the shortest time for which the fidelity is still at least 0.9.

7 One-click entanglement generation and swapping with imperfections

One-click entanglement generation and one-click swapping proved quite efficient under ideal conditions, but the situation looks very different once imperfections are taken into account. This chapter will explore the one-click generation and one-click swapping scheme with imperfections included.

The motivation for using an entanglement swapping protocol where acceptance is conditioned on two clicks lies in the decrease in the efficiency in the one-click swapping scheme once imperfections are taken into account.

7.1 One-click generation

While the detector modes for one-click entanglement generation and one-click swapping are the same as in Eq. (4.12) and (4.31) with and without imperfections we can no longer treat the measurement as a projective measurement. This is because for a measurement to be a projective measurement the measurement operators $P_m = M_m^\dagger M_m$ (see chapter 2.3 for an explanation of the operators M_m) must obey $P_m^2 = P_m$. When imperfections are included there are too many free variables that cannot be controlled during an experiment and the premise of a projective measurement no longer holds true.

Events that were not acceptable before, now has a non-zero chance of being accepted. Some examples are:

- No photon is emitted but there is a dark count causing the process to be accepted despite the system being in a wrong state.
- A photon is emitted but is lost in the fiber or simply not detected. If there is no dark count this causes the measurement outcome to be rejected and the process needs to be started over.
- Two photons are emitted, either from the same ensemble or one from each. If one of them is lost in transmission or simply not detected this causes the acceptance of an unwanted state. If both photons are detected the process is started over.

This means the measurement is best described by a Positive Operator Valued Measurement [POVM].

Suppose n photons reach the d_+ detector and m photons reach the d_- detector. Without imperfections only $n = 1, m = 0$ or $n = 0, m = 1$ were events that could result in an acceptance. To take the effect of imperfections into account there must also be a certain probability $\alpha(n, m)$ to accept other combinations of n and m[10]. Consider for example $n = 0$, $m = 0$. With $p_{dark} \neq 0$ this has a chance $p_{dark}(1 - p_{dark})$ of causing a click in d_+ and being accepted. Likewise for d_-.

In general the probability $\alpha_(n, m)$ of accepting an event where there are n photons in d_+ and m photons in d_- can be found. First all but one photon must be lost in order for the event to be accepted. This has probability $(1-\eta_{det})^{n+m-1}$. If there are n photons in the d_+ detector the probability that the remaining photon will be detected in d_+ must be $n \cdot \eta_{det}(1-p_{dark})$. Another possibility is the photon is lost but there is a dark count in d_+ with probability $(1 - \eta_{det})p_{dark}$. For the process to be accepted there must be no dark count in d_- which has the probability $(1 - p_{dark})$. The final expression for the probability $\alpha(n, m)$ to have a click in d_+ must thereby be given as:

$$\alpha(n, m) = (1 - \eta_{det})^{n+m-1}(n \cdot \eta_{det}(1 - p_{dark}) + (1 - \eta_{det})p_{dark})(1 - p_{dark}) \tag{7.1}$$

With this we can begin constructing the POVM describing the measurement.

Let $\rho_A = |\Psi\rangle \langle\Psi|_A$ with $|\Psi\rangle$ being the state from Eq. (5.11) and the label A denoting it as the state of ensemble A. Similarly ρ_B can be defined for ensemble B.

Define operators:

$$\Pi^{n,m}_{ph_a,ph_b} = |\phi\rangle \langle\phi|^{n,m}_{ph_a,ph_b}, \qquad |\phi\rangle^{n,m}_{ph_a,ph_b} = \frac{(d^\dagger_+)^n (d^\dagger_-)^m}{\sqrt{n!m!}} |\varnothing\rangle \tag{7.2}$$

The subscript ph_a, ph_b refers to the fact that the operators work on the photon modes of system A and B.

The entanglement generation measurement is performed by making a POVM on the photon modes of $\rho_A \otimes \rho_B$. An identity matrix is applied on the memory modes to represent that the measurement is not on that part of the system. The state after measurement given outcome

[10]Note n and m will be limited to at most have the value 2. We only consider the emission of at most two photons from the same ensemble, so in principle three or even even four photons could reach one of the detectors given a process with two ensembles. However to have $n > 2$ or $m > 2$ three or more photons in total would have had to have been emitted. The probability of such events is so small that it will be disregarded for the one-click schemes.

d_+ can be calculated using Eq. (2.21) giving the expression:

$$\rho'_{AB} = \frac{1}{p_+} \sum_{n,m=0}^{2} \alpha(n,m)(\mathbb{1}_{m_A,m_B} \otimes \Pi^{n,m}_{ph_a,ph_b})\rho_A \otimes \rho_B(\mathbb{1}_{m_A,m_B} \otimes \Pi^{n,m}_{ph_a,ph_b}) \tag{7.3}$$

The state of A and B each have memory modes as well as photon modes. After measuring on the photon modes we are mostly interested in the state of the memory modes of A and B. Therefore we can take the partial trace over the photon modes to get the state of the memory modes of A and B:

$$\rho'_{m_A,m_B} = Tr_{ph_a,ph_b}\Big(\frac{1}{p_+} \sum_{n,m=0}^{2} \alpha(n,m)(\mathbb{1}_{m_A,m_B} \otimes \Pi^{n,m}_{ph_a,ph_b})\rho_A \otimes \rho_B(\mathbb{1}_{m_A,m_B} \otimes \Pi^{n,m}_{ph_a,ph_b})\Big) \tag{7.4}$$

$$= \frac{1}{p_+} \sum_{n,m=0}^{2} \alpha(n,m) Tr_{ph_a,ph_b}\big((\mathbb{1}_{m_A,m_B} \otimes \Pi^{n,m}_{ph_a,ph_b})\rho_A \otimes \rho_B(\mathbb{1}_{m_A,m_B} \otimes \Pi^{n,m}_{ph_a,ph_b})\big) \tag{7.5}$$

$$= \frac{1}{p_+} \sum_{n,m=0}^{2} \alpha(n,m) Tr_{ph_a,ph_b}\big((\rho_A \otimes \rho_B)\Pi^{n,m}_{ph_a,ph_b}\big) \tag{7.6}$$

$$= \frac{\sum_{n,m=0}^{2} \alpha(n,m) \langle\phi|^{n,m}_{ph_a,ph_b} \rho_A \otimes \rho_B |\phi\rangle^{n,m}_{ph_a,ph_b}}{p_+} \tag{7.7}$$

Let c_x be the factor of some matrix element $c_x |m_A i_a\rangle \langle m'_A j_a| \otimes |m_B i_b\rangle \langle m'_B j_b|$ in the density matrix $\rho_A \otimes \rho_B$. m_A and m'_A refer to the number of excitations in the ensemble and i_a and j_a refer to the number of photons in the photon mode of system A. The contribution of this term must from Eq. (7.7) be given by:

$$c_x \sum_{n,m=0}^{2} \alpha(n,m) \langle\phi|^{n,m}_{ph_a,ph_b} |m_A i_a\rangle \langle m'_A j_a| \otimes |m_B i_b\rangle \langle m'_B j_b|\phi\rangle^{n,m}_{ph_a,ph_b} \tag{7.8}$$

$$= c_x |m_A m_B\rangle \langle m'_A m'_B| \sum_{n,m=0}^{2} \alpha(n,m) \langle\phi|^{n,m}_{ph_a,ph_b} |i_a\rangle \langle j_a| \otimes |i_b\rangle \langle j_b|\phi\rangle^{n,m}_{ph_a,ph_b} \tag{7.9}$$

From this it can be concluded that the state of the memory modes determine what the term contributes to in the resulting state, but the photonic modes determine the factor i.e. the size of the contribution. This means some factor dependent on i_a, j_a, i_b and j_b can be defined:

$$M[i_a, j_a, i_b, j_b] = \sum_{n,m=0}^{2} \alpha(n,m) \langle\phi|^{n,m}_{ph_a,ph_b} |i_a\rangle \langle j_a| \otimes |i_b\rangle \langle j_b|\phi\rangle^{n,m}_{ph_a,ph_b} \tag{7.10}$$

$$= \sum_{n,m=0}^{2} \alpha(n,m) \langle\phi|^{n,m}_{ph_a,ph_b} |i_a i_b\rangle \langle j_a j_b|\phi\rangle^{n,m}_{ph_a,ph_b} \tag{7.11}$$

Given the factor $M[i_a, j_a, i_b, j_b]$ the state after a measurement with outcome d_+ can be calculated. Let $\rho[m_A, m'_A, i_a, j_a]$ denote the matrix element at the position $|m_A\rangle \langle m'_A| \otimes |i_a\rangle \langle j_a|$ in the density matrix of A. The matrix element $\rho'[m_A, m'_A, m_B, m'_B]$ in the resulting density matrix is then given by:

$$\rho'[m_A, m'_A, m_B, m'_B] = \sum_{i_a,j_a,i_b,j_b=0}^{2} \rho[m_A, m'_A, i_a, j_a] \cdot \rho[m_B, m'_B, i_b, j_b] \cdot M[i_a, j_a, i_b, j_b] \tag{7.12}$$

To expand a bit on the expression for $M[i_a, j_a, i_b, j_b]$ consider the inner product $\langle\phi|^{n,m}_{ph_a,ph_b} |i_a i_b\rangle$. Recall from Eq. (7.2) $|\phi\rangle^{n,m}_{ph_a,ph_b} = \frac{(d_+^\dagger)^n (d_-^\dagger)^m}{\sqrt{n!m!}} |\varnothing\rangle$. $(d_+^\dagger)^n (d_-^\dagger)^m |\varnothing\rangle$ creates a polynomial with terms $\frac{(a^\dagger)^i (b^\dagger)^j}{\sqrt{n!m!}} |\varnothing\rangle = \frac{\sqrt{i!j!}}{\sqrt{n!m!}} c^{n,m}_{ij} |ij\rangle$ where $n + m = i + j$ and $c^{n,m}_{ij}$ is some coefficient. This means $\langle\phi|^{n,m}_{ph_a,ph_b} |i_a i_b\rangle = \frac{\sqrt{i_a! i_b!}}{\sqrt{n!m!}} c^{n,m}_{i_a i_b}$. Define $\mathit{coeff}[n, m, i_a, i_b] = \langle\phi|^{n,m}_{ph_a,ph_b} |i_a i_b\rangle = \frac{\sqrt{i_a! i_b!}}{\sqrt{n!m!}} c^{n,m}_{i_a i_b}$. The factor $M[i_a, j_a, i_b, j_b]$ can then be found to be:

$$M[i_a, j_a, i_b, j_b] = \sum_{n,m=0}^{2} \alpha(n,m) \cdot \mathit{coeff}[n, m, i_a, i_b] \mathit{coeff}[n, m, j_a, j_b] \tag{7.13}$$

As an example consider the term $c_0 |m_A\rangle \langle m'_A| \otimes |0\rangle \langle 0|_{ph_a} \otimes |m_B\rangle \langle m'_B| \otimes |0\rangle \langle 0|_{ph_b}$. From Eq. (7.9) in the sum only $n = 0$, $m = 0$ give a non-zero contribution. The contribution of this term must therefore be given by:

$$c_0 \sum_{n,m=0}^{2} \alpha(n,m) \langle\phi|^{n,m}_{ph_a,ph_b} |m_A\rangle \langle m'_A| \otimes |0\rangle \langle 0|_{ph_a} \otimes |m_B\rangle \langle m'_B| \otimes |0\rangle \langle 0|_{ph_b} |\phi\rangle^{n,m}_{ph_a,ph_b} \tag{7.14}$$

$$= c_0 |m_A m_B\rangle \langle m'_A m'_B| \sum_{n,m=0}^{2} \alpha(n,m) \langle\phi|^{n,m}_{ph_a,ph_b} |0\rangle \langle 0| \otimes |0\rangle \langle 0|\phi\rangle^{n,m}_{ph_a,ph_b} \tag{7.15}$$

$$c_0 \cdot p_{dark}(1 - p_{dark}) |m_A m_B\rangle \langle m'_A m'_B| \tag{7.16}$$

Doing this for each value of m_A, m'_A, m_B, m'_B between 0 and 2 the un-normalized density matrix ρ' of the resulting state can be calculated. Recall that from Eq. (7.7) we also needed to divide by p_+ to normalize the resulting density matrix to have trace 1. Recall p_+ was the probability to get outcome d_+. From Eq. (2.16) we have:

$$p_+ = Tr\Big(\sum_{n,m=0}^{2} \alpha(n,m)(\mathbb{1} \otimes \Pi^{n,m}_{ph_a,ph_b})\rho_A \otimes \rho_B(\mathbb{1} \otimes \Pi^{n,m}_{ph_a,ph_b}) \Big) \tag{7.17}$$

But $\sum_{n,m=0}^{2} \alpha(n,m)(\mathbb{1} \otimes \Pi^{n,m}_{ph_a,ph_b})\rho_A \otimes \rho_B(\mathbb{1} \otimes \Pi^{n,m}_{ph_a,ph_b}) = \rho'$ meaning we must have $p_+ = Tr(\rho')$. Thereby we have that the normalized density matrix of the resulting state given an outcome d_+ must be given by $\dfrac{\rho'}{Tr(\rho')}$.

What we have found is that with imperfections included there is a higher rejection probability as the probability of multi-photon errors become higher or photons can get lost or not detected causing no clicks. In addition to a higher time-cost the one-click entanglement generation scheme is burdened with a poorer fidelity of the final state, as now there is a probability that the resulting state is found in an unwanted state. This probability of the entanglement generation not producing the desired entanglement must be accounted for when looking at the subsequent swapping schemes.

7.2 One-click swapping

Having looked at the effect of imperfections on the entanglement generation scheme now we will look at the one-click swapping scheme. The first important difference is that going into the swapping process it can no longer be assumed that ensembles $A-B$ and $C-D$ are in an entangled state.

Recall that to perform entanglement swapping a measurement is carried out by reading out the excitations in the ensembles. This means instead of $\alpha(n,m)$ only being dependent on a detector efficiency η_{det} the read-out efficiency η_{read} must also be included. Let $\eta = \eta_{det} \cdot \eta_{read}$ be the combined read-out and detector efficiency. $\alpha(n,m)$ is then given by:

$$\alpha(n,m) = (1-\eta)^{n+m-1}(n \cdot \eta \cdot (1-p_{dark}) + (1-\eta)p_{dark})(1-p_{dark}) \tag{7.18}$$

In the same way as for the one-click generation scheme the resulting state of a one-click swapping scheme can be calculated with imperfections taken into account. Suppose we have some density matrix ρ_{ABCD} for the combined system of ensembles A, B, C and D in a one-click entanglement swapping scheme. In the same way we arrived at Eq. (7.3) but now with the measurement

operators applied on B and C and an identity matrix on A and D as that part of the system is not measured on:

$$\rho'_{ABCD} = \frac{1}{p_+} \sum_{n,m=0}^{2} \alpha(n,m)(\mathbb{1}_{AD} \otimes \Pi_{BC}^{n,m})\rho_{AB} \otimes \rho_{CD}(\mathbb{1}_{AD} \otimes \Pi_{BC}^{n,m}) \tag{7.19}$$

The state we are really interested in however is the state of A and D after measuring on B and C. We can get this by taking the partial trace over B and C like we took the partial trace over the photonic modes in the one-click entanglement generation scheme to arrive at Eq. (7.7):

$$\rho'_{AD} = Tr_{BC}\Big(\frac{1}{p_+} \sum_{n,m=0}^{2} \alpha(n,m)(\mathbb{1}_{AD} \otimes \Pi_{BC}^{n,m})\rho_{AB} \otimes \rho_{CD}(\mathbb{1}_{AD} \otimes \Pi_{BC}^{n,m})\Big) \tag{7.20}$$

$$= \frac{\sum_{n,m=0}^{2} \alpha(n,m) \left\langle\phi\right|_{BC}^{n,m} \rho_{AB} \otimes \rho_{CD} \left|\phi\right\rangle_{BC}^{n,m}}{p_+} \tag{7.21}$$

Like in Eq. (7.9) we can calculate the contribution of a term $c_x \left|m_A m_B\right\rangle \left\langle m'_A m'_B\right| \otimes \left|m_C m_D\right\rangle \left\langle m'_C m'_D\right|$:

$$\sum_{n,m=0}^{2} \alpha(n,m) \cdot c_x \left\langle\phi\right|_{BC}^{n,m} \left|m_A m_B\right\rangle \left\langle m'_A m'_B\right| \otimes \left|m_C m_D\right\rangle \left\langle m'_C m'_D\right|\left.\phi\right\rangle_{BC}^{n,m} \tag{7.22}$$

$$= c_x \left|m_A m_D\right\rangle \left\langle m'_A m'_D\right| \sum_{n,m=0}^{2} \alpha(n,m) \cdot \left\langle\phi\right|_{BC}^{n,m} \left|m_B\right\rangle \left\langle m'_B\right| \otimes \left|m_C\right\rangle \left\langle m'_C\right|\left.\phi\right\rangle_{BC}^{n,m} \tag{7.23}$$

As before only the modes that are subjected to the measurement control the contribution factor. This means again a factor, now only dependent on m_B, m'_B, m_C and m'_C can be defined:

$$M[m_B, m'_B, m_C, m'_C] = \sum_{n,m=0}^{2} \alpha(n,m) \cdot \left\langle\phi\right|_{BC}^{n,m} \left|m_B\right\rangle \left\langle m'_B\right| \otimes \left|m_C\right\rangle \left\langle m'_C\right|\left.\phi\right\rangle_{BC}^{n,m} \tag{7.24}$$

$$= \sum_{n,m=0}^{2} \alpha(n,m) \cdot \left\langle\phi\right|_{BC}^{n,m} \left|m_B m_C\right\rangle \left\langle m'_B m'_C\right|\left.\phi\right\rangle_{BC}^{n,m} \tag{7.25}$$

As before this expression can be expanded by considering the inner product $\left\langle\phi\right|_{BC}^{n,m} \left|m_B m_C\right\rangle$. We have $\left|\phi\right\rangle_{BC}^{n,m} = \frac{(d_+^\dagger)^n (d_-^\dagger)^m}{\sqrt{n!m!}} \left|\varnothing\right\rangle$ with $(d_+^\dagger)^n (d_-^\dagger)^m \left|\varnothing\right\rangle$ creating a polynomial, now with terms $\frac{(b^\dagger)^i (c^\dagger)^j}{\sqrt{n!m!}} \left|\varnothing\right\rangle = \frac{\sqrt{i!j!}}{\sqrt{n!m!}} c_{ij}^{n,m} \left|ij\right\rangle$. As before $n + m = i + j$ and $c_{ij}^{n,m}$ is some coefficient. This

means $\langle\phi|^{n,m}_{BC}|m_B m_C\rangle = \frac{\sqrt{m_B! m_B!}}{\sqrt{n!m!}} c^{n,m}_{m_B m_C}$. Define $\mathit{coeff}[n,m,m_b,m_C] = \langle\phi|^{n,m}_{BC}|m_B m_C\rangle = \frac{\sqrt{m_B! m_B!}}{\sqrt{n!m!}} c^{n,m}_{m_B m_C}$. The factor $M[m_B, m'_B, m_C, m'_C]$ can then be found to be:

$$M[m_B, m'_B, m_C, m'_C] = \sum_{n,m=0}^{2} \alpha(n,m) \cdot \mathit{coeff}[n,m,m_B,m_C]\mathit{coeff}[n,m,m'_B,m'_C] \tag{7.26}$$

Let $\rho[m_A, m'_A, m_B, m'_B]$ denote the matrix element at the position $|m_A\rangle\langle m'_A| \otimes |m_B\rangle\langle m'_B|$ in the density matrix ρ_{AB}. The matrix element $\rho'[m_A, m'_A, m_D, m'_D]$ in the resulting density matrix is then given by:

$$\rho'[m_A, m'_A, m_D, m'_D] = \sum_{m_B, m'_B, m_C, m'_C=0}^{2} \rho[m_A, m'_A, m_B, m'_B] \cdot \rho[m_C, m'_C, m_D, m'_D] \tag{7.27}$$

$$\cdot M[m_B, m'_B, m_C, m'_C] \tag{7.28}$$

Again we can consider what happens in special cases. For example consider $c_0 |m_A\rangle\langle m'_A| \otimes |0\rangle\langle 0| \otimes |0\rangle\langle 0| \otimes |m_D\rangle\langle m'_D|$:

$$\sum_{n,m=0}^{2} \alpha(n,m) \cdot c_0 \langle\phi|^{n,m}_{BC} |m_A\rangle\langle m'_A| \otimes |0\rangle\langle 0| \otimes |0\rangle\langle 0| \otimes |m_D\rangle\langle m'_D|\phi\rangle^{n,m}_{BC} \tag{7.29}$$

$$= c_0 |m_A m_D\rangle\langle m'_A m'_D| \sum_{n,m=0}^{2} \alpha(n,m) \cdot c_x \langle\phi|^{n,m}_{BC} |0\rangle\langle 0| \otimes |0\rangle\langle 0|\phi\rangle^{n,m}_{BC} \tag{7.30}$$

$$= c_0\, p_{dark}(1 - p_{dark}) |m_A m_D\rangle\langle m'_A m'_D| \tag{7.31}$$

The only real difference is the pre-factor c_0 which will be different between one-click entanglement generation and one-click entanglement swapping.

Doing this for each value of m_B, m'_B, m_C, m'_C between 0 and 2 the resulting un-normalized state ρ' can be calculated.

A similar argument to the one for the entanglement generation scheme can be made to arrive at an expression for p_+ for the swapping swapping scheme: $p_+ = Tr(\rho')$. This means similarly to before we have that the normalized resulting state of an entanglement swapping scheme with outcome d_+ is $\frac{\rho'}{Tr(\rho')}$.

To quantify the effect of imperfections on the one-click entanglement swapping scheme consider the possibilities of ending up with ensembles A and D being in the state $|00\rangle\langle 00|_{AD}$. There are a number of ways this can happen:

- Given no excitations in any of the four ensembles the swapping process could only be accepted if there was a dark count.
- Given only one excitation in either B or C the emitted photon could either be detected or if it is not detected there could be a dark count. It is worth noting that these events happen with only one of the ensemble pairs in a wrong state after entanglement generation.
- Given excitations in B and C one of the photons could not be detected. Note in this case none of the ensemble pairs are in a wrong state.
- ... and more

Imperfections clearly cause problems for the one-click swapping scheme, even if the entanglement generation was successful. Furthermore the one-click scheme is not designed in a way to catch these errors or at least to make them less likely. This means doing more swaps only decreases the fidelity of the resulting state further.

8 Two-click swapping

Due to imperfections there were many possibilities for the one-click swapping scheme to produce a wrong state. The scheme was not designed in a way to negate certain imperfections or make them less likely to cause an accept.

In this chapter more advanced swapping schemes which require clicks in two detectors will be introduced motivated by the need to limit the effect of imperfections.

There are two different types of two-click swapping methods that will be discussed in this thesis. This chapter will discuss both of them and then compare the two to find if one is to be preferred over the other.

8.1 Type 1 two-click swapping

The first type two-click swapping scheme uses four pairs of entangled ensembles[11]: $\rho_{AhBh} \otimes \rho_{ChDh} \otimes \rho_{AvBv} \otimes \rho_{CvDv}$. Then ensembles Bh, Ch, Bv and Cv causing the emission of anti-stokes photons. These are then taken trough beam-splitters, combined at a central station, sent trough another pair of beam-splitters and lastly detected in modes: [4]

$$d_\pm = \frac{1}{2}(b_h + b_v \pm c_h \mp c_v), \qquad \tilde{d}_\pm = \frac{1}{2}(\pm b_h \mp b_v + c_h + c_v) \tag{8.1}$$

An illustration of the setup can be found in figure 13 below.

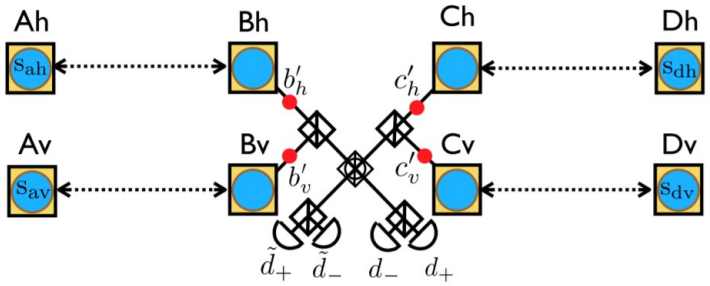

Figure 13: The setup of the first type of entanglement swapping conditioned on two clicks. Four pairs of entangled ensembles are used, and one ensemble from each pair is then read out. The emitted anti-stokes photons are then sent through polarizing beam-splitters and combined at a central station. Acceptance is conditioned on a click in certain pairs of two of the four detectors. [4]

[11]For the protocols discussed in this paper the entanglement will be created using one-click entanglement generation

To accept this entanglement swapping process there must be click in *either* d_+ or d_- *and* $\tilde{d}_+$ or $\tilde{d}_-$. Thereby there are only four combinations resulting in the process being accepted. Each of which requires two clicks. An example of expanding an acceptable combination gives the following expression:

$$d_+\tilde{d}_+ = \frac{1}{4}(2b_hc_h + 2b_vc_v + b_h^2 - b_v^2 + c_h^2 - c_v^2) \tag{8.2}$$

From this we can determine what configurations cause an acceptable event provided there are no other imperfections. An accept can be caused by the emission of a photon from Bh and Ch or Bv and Cv. Another option is the emission of two photons from any of the four ensembles provided they were emitted from the same one.

This means given ideal conditions the detection of a photon in d_+ and $\tilde{d}_+$ would project the state of Ah, Dh, Av and Dv into the entangled state:

$$|\psi\rangle_{AhDhAvDv} = \frac{1}{\sqrt{2}}(|11\rangle_{AhDh} \otimes |00\rangle_{AvDv} + |00\rangle_{AhDh} \otimes |11\rangle_{AvDv}) \tag{8.3}$$

This was given the outcome $d_+\tilde{d}_+$. Similar observations can be made for $d_+\tilde{d}_-$, $d_-\tilde{d}_+$ and $d_-\tilde{d}_-$.

The measurement is made on Bh, Ch, Bv and Cv so we can assume some measurement operator $M = |\phi\rangle\langle\phi|_{BhChBvCv}$. Just as we arrived at Eq. (7.3) and (7.19) we get from Eq. (2.21) that the resulting state is given by:

$$\rho'_{AhBhChDhAvBvCvDv} = \frac{1}{p_+}\sum_{\substack{n_1,n_2\\n_3,n_4}=0}^{2} \alpha(n_1,n_2,n_3,n_4) \tag{8.4}$$
$$\left(\mathbb{1}_{AhDhAvDv}\otimes\Pi^{n_1,n_2,n_3,n_4}_{BhChBvCv}\right)\frac{\rho_{AhBh}\otimes\rho_{ChDh}\otimes\rho_{AvBv}\otimes\rho_{CvDv}}{p_+}\left(\mathbb{1}_{AhDhAvDv}\otimes\Pi^{n_1,n_2,n_3,n_4}_{BhChBvCv}\right)$$

Seeing as it is the state of Ah, Dh, Av and Dv we are interested in the partial trace is taken over Bh, Ch, Bv and Cv like it was with the photon modes in Eq. (7.7) and with the memory modes of B and C in (7.20)

$$\rho'_{AhDhAvDv} = Tr_{BhChBvCv}\Big(\sum_{\substack{n_1,n_2\\n_3,n_4=0}}^{2} \alpha(n_1,n_2,n_3,n_4)\big(\mathbb{1}_{AhDhAvDv} \otimes \Pi^{n_1,n_2,n_3,n_4}_{BhChBvCv}\big) \tag{8.5}$$

$$\frac{\rho_{AhBh} \otimes \rho_{ChDh} \otimes \rho_{AvBv} \otimes \rho_{CvDv}}{p_+}\big(\mathbb{1}_{AhDhAvDv} \otimes \Pi^{n_1,n_2,n_3,n_4}_{BhChBvCv}\big)\Big)$$

$$= \frac{1}{p_+} \sum_{\substack{n_1,n_2\\n_3,n_4=0}}^{2} \alpha(n_1,n_2,n_3,n_4) \tag{8.6}$$

$$\langle\phi^{n_1,n_2,n_3,n_4}|_{BhChBvCv}\, \rho_{AhBh} \otimes \rho_{ChDh} \otimes \rho_{AvBv} \otimes \rho_{CvDv}\, |\phi^{n_1,n_2,n_3,n_4}\rangle_{BhChBvCv}$$

This leads to a very similar expression for the contribution of a term $c_n \left|m_{Ah}m_{Bh}\right\rangle \left\langle m'_{Ah}m'_{Bh}\right| \otimes \left|m_{Ch}m_{Dh}\right\rangle \left\langle m'_{Ch}m'_{Dh}\right| \otimes \left|m_{Av}m_{Bv}\right\rangle \left\langle m'_{Av}m'_{Bv}\right| \otimes \left|m_{Cv}m_{Dv}\right\rangle \left\langle m'_{Cv}m'_{Dv}\right|$ as Eq. (7.9) and (7.23):

The differences begin when evaluating the contribution of specific terms. As an example take the contribution of a term $c_x \left|m_{Ah}m_{Bh}\right\rangle \left\langle m'_{Ah}m'_{Bh}\right| \otimes \left|m_{Ch}m_{Dh}\right\rangle \left\langle m'_{Ch}m'_{Dh}\right| \otimes \left|m_{Av}m_{Bv}\right\rangle \left\langle m'_{Av}m'_{Bv}\right| \otimes \left|m_{Cv}m_{Dv}\right\rangle \left\langle m'_{Cv}m'_{Dv}\right|$:

$$\sum_{n_1,n_2,n_3,n_4=0}^{2} \alpha(n_1,n_2,n_3,n_4) \cdot c_x \left\langle\phi^{n_1,n_2,n_3,n_4}\right|_{BhChBvCv} \left|m_{Ah}m_{Bh}\right\rangle \left\langle m'_{Ah}m'_{Bh}\right| \otimes \tag{8.7}$$

$$\left|m_{Ch}m_{Dh}\right\rangle \left\langle m'_{Ch}m'_{Dh}\right| \otimes \left|m_{Av}m_{Bv}\right\rangle \left\langle m'_{Av}m'_{Bv}\right| \otimes \left|m_{Cv}m_{Dv}\right\rangle \left\langle m'_{Cv}m'_{Dv}\right| \ \left|\phi^{n_1,n_2,n_3,n_4}\right\rangle_{BhChBvCv}$$

$$= c_x \left|m_{Ah}m_{Dh}m_{Av}m_{Dv}\right\rangle \left\langle m'_{Ah}m'_{Dh}m'_{Av}m'_{Dv}\right| \sum_{n_1,n_2,n_3,n_4=0}^{2} \alpha(n_1,n_2,n_3,n_4) \tag{8.8}$$

$$\left\langle\phi^{n_1,n_2,n_3,n_4}\right|_{BhChBvCv} \left|m_{Bh}\right\rangle \left\langle m'_{Bh}\right| \otimes \left|m_{Ch}\right\rangle \left\langle m'_{Ch}\right| \otimes \left|m_{Bv}\right\rangle \left\langle m'_{Bv}\right| \otimes \left|m_{Cv}\right\rangle \left\langle m'_{Cv}\right| \ \left|\phi^{n_1,n_2,n_3,n_4}\right\rangle_{BhChBvCv}$$

Again only the modes which are measured on influence the contribution factor. This means we can as before consider a special case namely the term $\left|m_{Ah}\right\rangle \left\langle m'_{Ah}\right| \otimes \left|0\right\rangle \left\langle 0\right|_{Bh} \otimes \left|0\right\rangle \left\langle 0\right|_{Ch} \otimes \left|m_{Dh}\right\rangle \left\langle m'_{Dh}\right| \otimes \left|m_{Av}\right\rangle \left\langle m'_{Av}\right| \otimes \left|0\right\rangle \left\langle 0\right|_{Bv} \otimes \left|0\right\rangle \left\langle 0\right|_{Cv} \left|m_{Dv}\right\rangle \left\langle m'_{Dv}\right|$.

Suppose n_1 photons reach the d_+ detector, n_2 photons reach the d_-, n_3 photons reach the $\tilde{d}_+$ detector and n_4 photons reach the $\tilde{d}_-$ detector. There is only a contribution if $\left|\phi\right\rangle_{BhChBvCv} = \left|0000\right\rangle_{BhChBvCv}$ meaning $n_1 = n_2 = n_3 = n_4 = 0$. The probability of accepting this event given that in this swapping scheme acceptance is conditioned on two clicks is given by $p_{dark}^2(1-p_{dark})^2$. This means we have:

$$\sum_{n_1,n_2,n_3,n_4=0}^{2} \alpha(n_1,n_2,n_3,n_4)\cdot c_0 \left\langle \phi^{n_1,n_2,n_3,n_4}\right|_{BhChBvCv} |m_{Ah}0\rangle \langle m'_{Ah}0| \otimes |0m_{Dh}\rangle \langle 0m'_{Dh}| \otimes \tag{8.9}$$
$$|m_{Av}0\rangle \langle m'_{Av}0| \otimes |0m_{Dv}\rangle \langle 0m'_{Dv}| \ \left|\phi^{n_1,n_2,n_3,n_4}\right\rangle_{BhChBvCv}$$
$$= c_x \, |m_{Ah}m_{Dh}m_{Av}m_{Dv}\rangle \langle m'_{Ah}m'_{Dh}m'_{Av}m'_{Dv}| \sum_{n_1,n_2,n_3,n_4=0}^{2} \alpha(n_1,n_2,n_3,n_4) \tag{8.10}$$
$$\left\langle \phi^{n_1,n_2,n_3,n_4}\right|_{BhChBvCv} |0\rangle \langle 0| \otimes |0\rangle \langle 0| \otimes |0\rangle \langle 0| \otimes |0\rangle \langle 0| \ \left|\phi^{n_1,n_2,n_3,n_4}\right\rangle_{BhChBvCv}$$
$$= c_0 \, p_{dark}^2 (1-p_{dark})^2 \, |m_{Ah}m_{Dh}m_{Av}m_{Dv}\rangle \langle m'_{Ah}m'_{Dh}m'_{Av}m'_{Dv}| \tag{8.11}$$

Taking another example consider the contribution of a term $|m_{Ah}1\rangle \langle m'_{Ah}1| \otimes |1m_{Dh}\rangle \langle 1m'_{Dh}| \otimes |m_{Av}0\rangle \langle m'_{Av}0| \otimes |0m_{Dv}\rangle \langle 0m'_{Dv}|$. There is only a contribution if for $(d_+)^{n_1}(d_-)^{n_2}(\tilde{d}_+)^{n_3}(\tilde{d}_-)^{n_4}$ we have:

$$\begin{aligned}
&n_1 = n_3 = 1, \quad n_2 = n_4 = 0\\
&n_2 = n_4 = 1, \quad n_1 = n_3 = 0\\
&n_1 = 2, \quad n_2 = n_3 = n_4 = 0\\
&n_2 = 2, \quad n_1 = n_3 = n_4 = 0\\
&n_3 = 2, \quad n_1 = n_2 = n_4 = 0\\
&n_4 = 2, \quad n_1 = n_2 = n_3 = 0
\end{aligned}$$

Each of these must be calculated as in Eq. (8.9) and added together to get the total contribution.

Let $\alpha(n_1,n_2,n_3,n_4)$ be the probability of getting a click in the d_+ and $\tilde{d_+}$ detectors given the situation $(d_+)^{n_1}(d_-)^{n_2}(\tilde{d}_+)^{n_3}(\tilde{d}_-)^{n_4}$. It must be given by:

$$\begin{aligned}
\alpha(n_1,n_2,n_3,n_4) = (1-\eta)^{n_1+n_2+n_3+n_4-2}(n_1\cdot\eta\cdot(1-p_{dark})+(1-\eta)p_{dark}) \\
\cdot(n_3\cdot\eta\cdot(1-p_{dark})+(1-\eta)p_{dark})(1-p_{dark})^2
\end{aligned} \tag{8.12}$$

Let $c_{i_1i_2i_3i_4}^{n_1,n_2,n_3,n_4}$ be the coefficient of $(b_h)^{i_1}(c_h)^{i_2}(b_v)^{i_3}(c_v)^{i_4}$ from the polynomial $(d_+)^{n_1}(d_-)^{n_2}(\tilde{d}_+)^{n_3}(\tilde{d}_-)^{n_4}$

Define $coeff[n_1,n_2,n_3,n_4,\ i_1,i_2,i_3,i_4] = \dfrac{\sqrt{i_1!i_2!i_3!i_4!}}{\sqrt{n_1!n_2!n_3!n_4!}} c_{i_1i_2i_3i_4}^{n_1,n_2,n_3,n_4}$.

The element $M[i_1,j_1,i_2,j_2,i_3,j_3,i_4,j_4] = \sum_{n_1,n_2,n_3,n_4=0}^{2} \alpha(n_1,n_2,n_3,n_4) \left\langle \phi^{n_1,n_2,n_3,n_4}\right|_{BhChBvCv} |i_1\rangle \langle j_1| \otimes |i_2\rangle \langle j_2| \otimes |i_3\rangle \langle j_3| \otimes |i_4\rangle \langle j_4| \ \left|\phi^{n_1,n_2,n_3,n_4}\right\rangle_{BhChBvCv}$ in the measurement operator is then given by:

$$M[i_1,j_1,i_2,j_2,i_3,j_3,i_4,j_4] = \sum_{n_1,n_2,n_3,n_4=0}^{2} \alpha(n_1,n_2,n_3,n_4) \tag{8.13}$$
$$\cdot\, coeff[n_1,n_2,n_3,n_4,\ i_1,i_2,i_3,i_4] \cdot coeff[n_1,n_2,n_3,n_4,\ j_1,j_2,j_3,j_4]$$

The matrix element $\rho'[m_{Ah}, m'_{Ah}, m_{Dh}, m'_{Dh}, m_{Av}, m'_{Av}, m_{Dv}, m'_{Dv}]$ at position $|m_{Ah}m_{Dh}m_{Av}m_{Dv}\rangle \langle m'_{Ah}m'_{Dh}m'_{Av}m'_{Dv}|$ in the resulting density matrix can then be calculated as:

$$\rho'[m_{Ah}, m'_{Ah}, m_{Dh}, m'_{Dh}, m_{Av}, m'_{Av}, m_{Dv}, m'_{Dv}] \tag{8.14}$$
$$= \sum_{\substack{m_{Bh},m'_{Bh},\, m_{Ch},m'_{Ch},\\ m_{Bv},m'_{Bv},\, m_{Cv},m'_{Cv}=0}}^{2} \rho[m_{Ah}, m'_{Ah}, m_{Bh}, m'_{Bh}] \cdot \rho[m_{Ch}, m'_{Ch}, m_{Dh}, m'_{Dh}] \tag{8.15}$$
$$\cdot\, \rho[m_{Av}, m'_{Av}, m_{Bv}, m'_{Bv}] \cdot \rho[m_{Cv}, m'_{Cv}, m_{Dv}, m'_{Dv}]$$
$$\cdot\, M[m_{Bh}, m'_{Bh}, m_{Ch}, m'_{Ch}, m_{Bv}, m'_{Bv}, m_{Cv}, m'_{Cv}]$$

In this way all the elements in the un-normalized density matrix of the resulting state can be calculated. As for the one-click schemes the normalization factor p_+ can be found as $Tr(\rho')$. This means the resulting normalized state after a measurement with outcome $d_+\tilde{d}_+$ can be found as $\dfrac{\rho'}{Tr(\rho')}$.

8.2 Type 2 two-click swapping

The setup of type 2 two-click swapping is very similar to type 1. It also uses 4 pairs of entangled ensembles and four detectors. Measurements are again conditioned on getting a click in two detectors as well. The setup can be seen in figure 14 below.

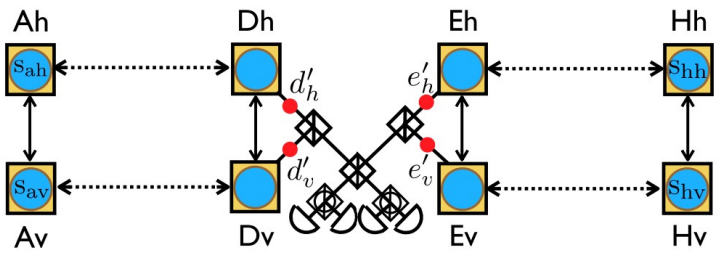

Figure 14: The setup of the second type of entanglement swapping conditioned on two clicks. Completely similar to the first type except the modes of the detectors are different. [4]

Again an accept occurs only if a photon is detected in d_+ or d_- *and* $\tilde{d}_+$ or $\tilde{d}_-$. The only difference between type 1 and type 2 two-click swapping are the detector modes which for type 2 are: [4]

$$d_\pm = \frac{1}{\sqrt{2}}(b_h \pm c_v), \qquad \tilde{d}_\pm = \frac{1}{\sqrt{2}}(c_h \pm b_v) \tag{8.16}$$

An example of expanding an acceptable combination gives the following expression:

$$d_+\tilde{d}_+ = \frac{1}{2}(b_h c_h + b_v c_v + b_h b_v + c_h c_v) \tag{8.17}$$

In contrast to type 1 which could get accepted if two photons were emitted from the same ensemble, type 2 can get accepted if two photons are emitted from the same side but from different ensembles i.e. Bh and Bv or Ch and Cv. Doing type 1 two-click swapping first should ideally eliminate the possibility of getting two photons from the same side. However due to imperfections it is still possible for this error to occur.

Given ideal conditions the detection of a photon in d_+ and $\tilde{d}_+$ would project the state of Ah, Dh, Av and Dv into the entangled state:

$$|\psi\rangle_{AhDhAvDv} = \frac{1}{\sqrt{2}}(|11\rangle_{AhDh} \otimes |00\rangle_{AvDv} + |00\rangle_{AhDh} \otimes |11\rangle_{AvDv}) \tag{8.18}$$

This was given the outcome $d_+\tilde{d}_+$. Similar observations can be made for $d_+\tilde{d}_-$, $d_-\tilde{d}_+$ and $d_-\tilde{d}_-$.

Given only the detector modes differ between the two types of two-click swaps, it can be concluded that equations (8.4) up to and including (8.8) are completely equivalent for type 1 and type 2 two-click swapping. The differences begin when calculating the inner products $\langle\phi^{n_1,n_2,n_3,n_4}|_{BhChBvCv}\,|m_{Bh}m_{Ch}m_{Bv}m_{Cv}\rangle$ and $\langle m'_{Bh}m'_{Ch}m'_{Bv}m'_{Cv}|\ |\phi^{n_1,n_2,n_3,n_4}\rangle_{BhChBvCv}$.

Consider the contribution of the term $|m_{Ah}\rangle\langle m'_{Ah}| \otimes |1\rangle\langle 1|_{Bh} \otimes |1\rangle\langle 1|_{Ch} \otimes |m_{Dh}\rangle\langle m'_{Dh}| \otimes |m_{Av}\rangle\langle m'_{Av}| \otimes |0\rangle\langle 0|_{Bv} \otimes |0\rangle\langle 0|_{Cv}\,|m_{Dv}\rangle\langle m'_{Dv}|$. With the modes as described in Eq. (8.16) this term only gives a contribution if for $(d_+)^{n_1}(d_-)^{n_2}(\tilde{d}_+)^{n_3}(\tilde{d}_-)^{n_4}$ we have:

$$\begin{aligned} n_1 = n_3 = 1, \quad n_2 = n_4 = 0 \\ n_2 = n_4 = 1, \quad n_1 = n_3 = 0 \end{aligned}$$

As before each of these must be calculated and added together to get the total contribution.

The probability $\alpha(n_1, n_2, n_3, n_4)$ of getting a click in d_+ and $\tilde{d}_+$ will still be given by Eq. (8.12).

Let $c_{i_1 i_2 i_3 i_4}^{n_1,n_2,n_3,n_4}$ be the coefficient of $(b_h)^{i_1}(c_h)^{i_2}(b_v)^{i_3}(c_v)^{i_4}$ from the polynomial $(d_+)^{n_1}(d_-)^{n_2}(\tilde{d}_+)^{n_3}(\tilde{d}_-)^{n_4}$. Again define $\mathit{coeff}[n_1, n_2, n_3, n_4,\ i_1, i_2, i_3, i_4] = \frac{\sqrt{i_1!i_2!i_3!i_4!}}{\sqrt{n_1!n_2!n_3!n_4!}} c_{i_1 i_2 i_3 i_4}^{n_1,n_2,n_3,n_4}$.

The element $M[i_1, j_1, i_2, j_2, i_3, j_3, i_4, j_4] = \sum_{n_1,n_2,n_3,n_4=0}^{2} \alpha(n_1, n_2, n_3, n_4) \langle \phi^{n_1,n_2,n_3,n_4}|_{BhChBvCv} |i_1\rangle \langle j_1| \otimes |i_2\rangle \langle j_2| \otimes |i_3\rangle \langle j_3| \otimes |i_4\rangle \langle j_4|\ |\phi^{n_1,n_2,n_3,n_4}\rangle_{BhChBvCv}$ in the measurement operator is then as in type 1 two-click swapping given by:

$$M[i_1, j_1, i_2, j_2, i_3, j_3, i_4, j_4] = \sum_{n_1,n_2,n_3,n_4=0}^{2} \alpha(n_1, n_2, n_3, n_4) \tag{8.19}$$
$$\cdot\, \mathit{coeff}[n_1, n_2, n_3, n_4,\ i_1, i_2, i_3, i_4] \cdot \mathit{coeff}[n_1, n_2, n_3, n_4,\ j_1, j_2, j_3, j_4]$$

Thereby the matrix element $\rho'[m_{Ah}, m'_{Ah}, m_{Dh}, m'_{Dh}, m_{Av}, m'_{Av}, m_{Dv}, m'_{Dv}]$ at position $|m_{Ah} m_{Dh} m_{Av} m_{Dv}\rangle \langle m'_{Ah} m'_{Dh} m'_{Av} m'_{Dv}|$ in the resulting density matrix can then again be calculated as:

$$\rho'[m_{Ah}, m'_{Ah}, m_{Dh}, m'_{Dh}, m_{Av}, m'_{Av}, m_{Dv}, m'_{Dv}] \tag{8.20}$$
$$= \sum_{\substack{m_{Bh},m'_{Bh},\, m_{Ch},m'_{Ch},\\ m_{Bv},m'_{Bv},\, m_{Cv},m'_{Cv}=0}}^{2} \rho[m_{Ah}, m'_{Ah}, m_{Bh}, m'_{Bh}] \cdot \rho[m_{Ch}, m'_{Ch}, m_{Dh}, m'_{Dh}] \tag{8.21}$$
$$\cdot\, \rho[m_{Av}, m'_{Av}, m_{Bv}, m'_{Bv}] \cdot \rho[m_{Cv}, m'_{Cv}, m_{Dv}, m'_{Dv}]$$
$$\cdot\, M[m_{Bh}, m'_{Bh}, m_{Ch}, m'_{Ch}, m_{Bv}, m'_{Bv}, m_{Cv}, m'_{Cv}]$$

In this way all the elements in the un-normalized density matrix of the resulting state can be calculated. As before with $p_+ = Tr(\rho')$ the resulting normalized state after a measurement with outcome $d_+\tilde{d}_+$ can be found as $\frac{\rho'}{Tr(\rho')}$.

8.3 Comparison of type 1 and type 2

Comparing the expansions from Eq. (8.2) and (8.17) it can be concluded that the two types of two-click swaps are vulnerable to different types of errors. Type 1 is vulnerable to the multi-photon error arising when an ensemble emits two photons. Type 2 is vulnerable to the error that arises when photons are emitted from the same side in the setup. As mentioned this thesis explores the effect of the multi-photon error caused by the emission of two photons from the same source. This is done by varying the probability the source has of this particular error. For this reason the type 1 swap will be expected to outperform type 2 when the probability of this particular multi-photon error is low.

9 Protocols

The protocols that will be focused on in this thesis are the Jiang protocol as desccribed in [4] and [5] and a version of the Jiang protocol where only the first type of two-click swap is used for swappings - this version will be referred to as modified Jiang. The source state used in the protocols will also be changed as part of the purpose of this thesis thesis is to explore the effect the $|22\rangle$ term has on the performance of the protocols. A factor will be added to control and vary the size of the $|22\rangle$ term. When the factor added is 0 it will be referred to as having $dim = 2$. When the factor added is 1 it will be refer

9.1 Standard Jiang protocol

The standard Jiang protocol uses one-click entanglement generation, the two-click swap mentioned in section 8.1 for the first swap and the two-click swap mentioned in section 8.2 for all subsequent swaps.

Plotting the fidelity of the resulting state of the standard Jiang protocol as a function of p for various values of n and with parameters $L = 1000$, $\eta_{det} = \eta_{read} = 0.9$, $p_{dark} = 0$ and $dim = 3$ produced the graphs found in figure 15.

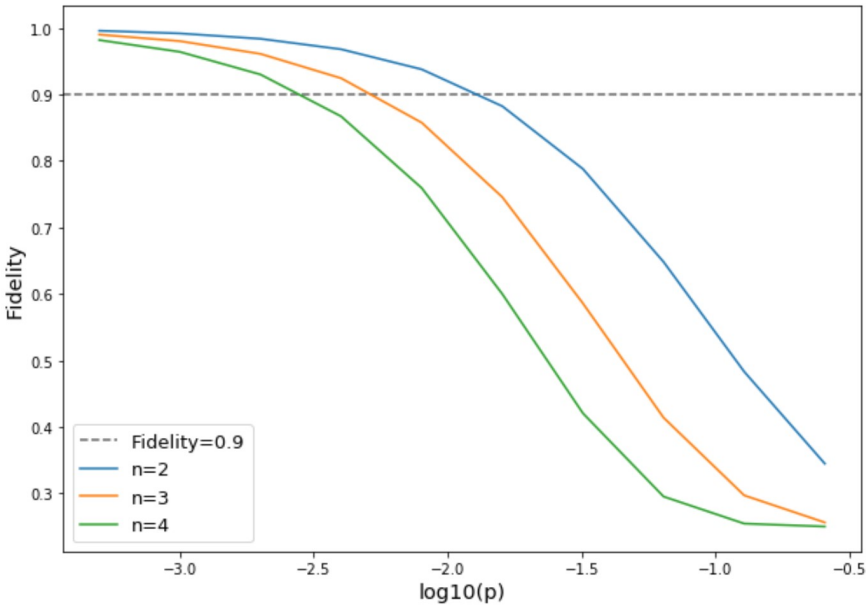

Figure 15: A plot of fidelity as a function of p for different values of n and with parameters $L = 1000$, $\eta_{det} = \eta_{read} = 0.9$, $p_{dark} = 0$ and $dim = 3$. Fidelity decreases with higher p and more swaps.

The higher the probability p of emitting photons, the higher the probability of multi-photon errors. If the ensembles have a high probability of emitting more than one photon chances are

due to photon loss or other imperfections that a wrong state may be accepted. Thereby the fidelity gets worse with higher values of p. Furthermore with more swaps there are more steps where there are opportunities for errors to occur. For this reason it is also natural to see a lower fidelity with higher nesting levels. These observations are exactly what can be found in figure 15.

Likewise plotting time as a function of p for different values of n and the same parameters as before produced the graphs found in figure 16.

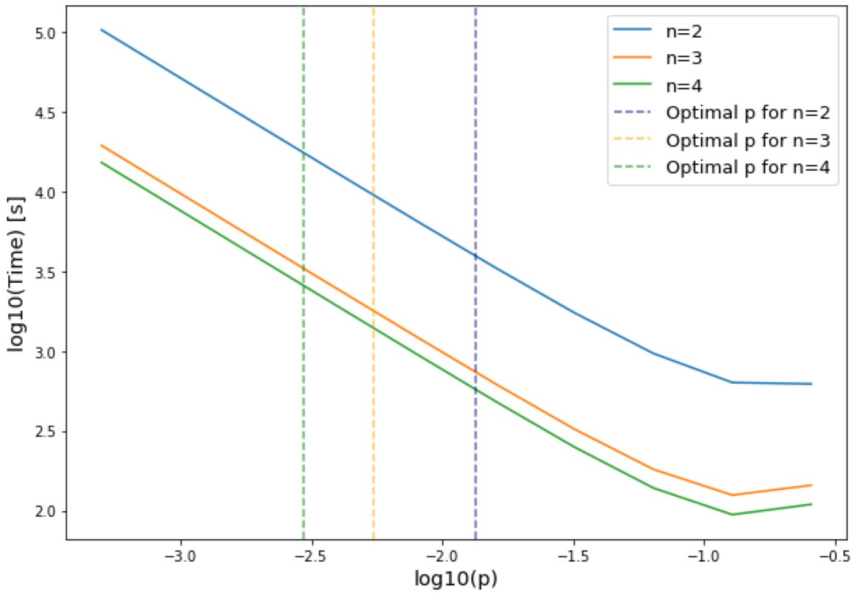

Figure 16: A plot of time as a function of p for different values of n and with parameters $L = 1000$, $\eta_{det} = \eta_{read} = 0.9$, $p_{dark} = 0$ and $dim = 3$. Time is shorter for higher p and more swaps.

With higher values of p it is faster to actually get an emission of a photon and thereby have a chance to accept an entanglement generation step. Of course if the probability of emitting more than one photon also increases for higher values of p. Because of this at a certain point it is not better to increase the value of p considering the protocol has a greater chance of being started over due to getting multiple clicks. It is also faster with higher nesting levels. This is simply because the greatest risk of photon loss is during entanglement generation. By making the elemental distance L_0 between links smaller the risk of photon loss also gets smaller. With a smaller probability of losing the photon the probability of accepting the entanglement generation step increases. This is exactly what we see in figure 16.

In conclusion what we can gain from figure 15 and 16 is that there is a trade-off between fidelity and time as p gets larger. The fidelity decreases, but in contrast the time gets shorter at least up to a certain point. It is also worth noting that the time is better with more swaps, but the fidelity is worse - again another trade-off.

Using the Newton-Raphson optimization algorithm described in chapter 6.1 the value of p for each n for which the fidelity is exactly 0.9 can be found. As argued this must be the optimal value of p for the given parameters. That is it must the the value of p for which the time is shortest. Calculating this for the parameters from before $L = 1000$, $\eta_{det} = \eta_{read} = 0.9$, $p_{dark} = 0$ and $dim = 3$ results in $p = 1.3 \cdot 10^{-2}$.

In figure 17 is a plot of the optimal time as a function of distance for $n = 2$, $n = 3$ and $n = 4$.

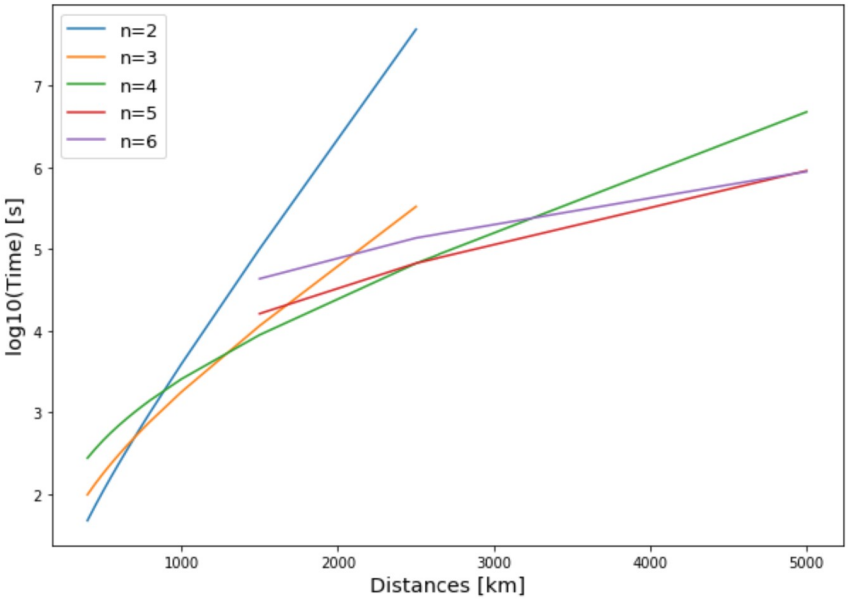

Figure 17: A plot of the optimal time as a function of distance for $n = 2$, $n = 3$ and $n = 4$ for $dim = 3$.

As seen from the graphs in figure 17 the optimal value of n changes with distance. For distances under about 700 km $n = 2$ has the lowest time. For distances between 700 km and about 1300 km $n = 3$ is best and so on. The further the distance the more swaps are needed to have the lowest possible time.

9.2 Modified Jiang

Another protocol worth considering is the modified Jiang protocol. The modified Jiang protocol uses one-click entanglement generation and the two-click swap mentioned in section 8.1 for all swaps.

9.2.1 Comparison with standard Jiang

As done for the standard Jiang protocol the fidelity and time can be plotted as a function of p for various values of n and using the parameters from previously: $L = 1000$ km, $\eta_{det} = \eta_{read} = 0.9$,

$p_{dark} = 0$ and $dim = 3$. Comparing the resulting graphs with the ones from the standard Jiang protocol produces the plots found in figure 18 and 19.

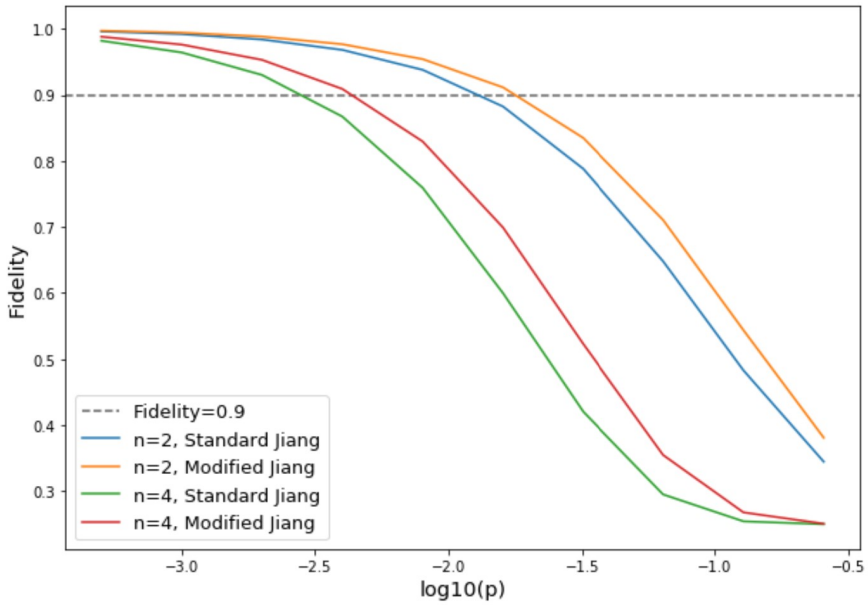

Figure 18: Comparative plots of the fidelity as a function p. Different values of n were plotted for fixed parameters $L = 1000$ km, $\eta_{det} = \eta_{read} = 0.9$, $p_{dark} = 0$ and $dim = 3$.

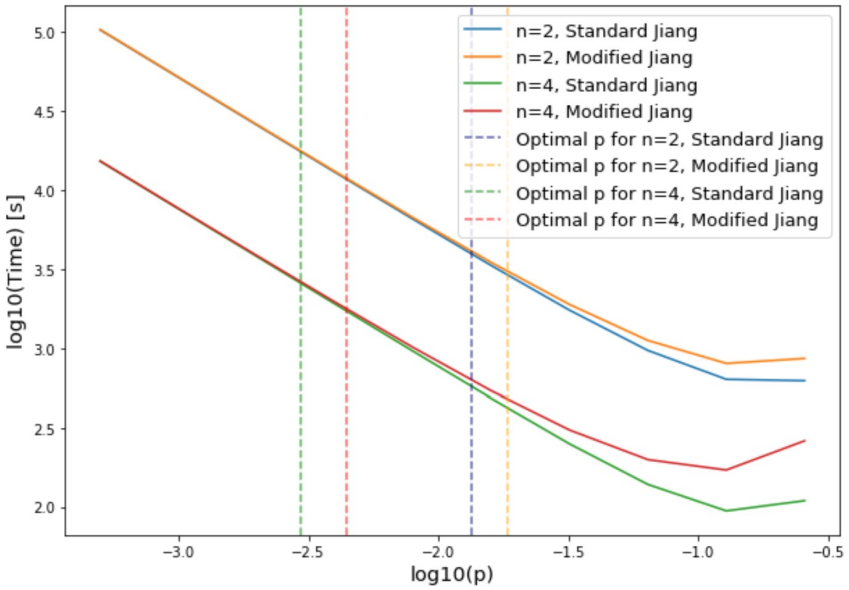

Figure 19: Comparative plots of the time as a function p. Different values of n were plotted for fixed parameters $L = 1000$ km, $\eta_{det} = \eta_{read} = 0.9$, $p_{dark} = 0$ and $dim = 3$.

From the comparison of the standard Jiang and modified Jiang protocols seen in figures 18 and 19 it can be concluded that the modified Jiang protocol takes the shortest amount of time.

This is due to the fact that the fidelity of the resulting final state is higher in the modified Jiang protocol. Because a higher p can be chosen and still have a resulting state with fidelity 0.9, combined with the fact that time as a function of p is practically equivalent for the two protocols up to a certain point means the modified Jiang Protocol is strictly better.

One might wonder why the modified Jiang protocol performs worse in figure 19 for higher p. This is due to the fact that the modified Jiang protocol is better at catching the multi-photon errors. Catching unwanted states results in the process being started over, but the fidelity of the final state when the whole process is eventually accepted is higher.

The optimal value of time was found over all values of n for a number of different distances for parameters $L = 1000$ km, $\eta_{det} = \eta_{read} = 0.9$, $p_{dark} = 0$. The optimal time was then plotted as a function of distance for the standard and modified Jiang protocols for $dim = 3$ and $dim = 2$. The resulting plot can be seen in figure 20.

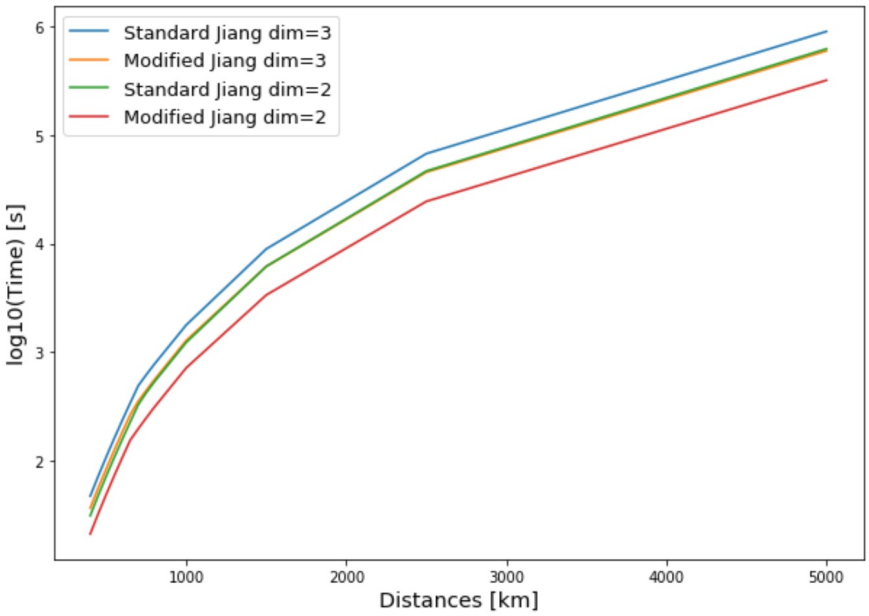

Figure 20: Comparative plot of the optimal time as a function of distance for the standard and modified Jiang protocols for $dim = 2$ and $dim = 3$.

From these graphs it is also clear that the modified Jiang protocol works best for both $dim = 3$ and $dim = 2$.

It is perhaps not obvious why there would be a difference between the standard and the modified Jiang protocols for $dim = 2$ considering the term $|22\rangle$ is neglected in this case. There are however other ways to have multi-photon errors than simply the emission of two photons from a single ensemble. It may be that one photon is emitted from two ensembles or in the case of the two-click swapping even three or four ensembles. This means there is still an advantage to

using the modified Jiang protocol even when $dim = 2$.

For this reason the modified Jiang protocol will be the one used when exploring the effect of imperfections on the performance of quantum repeater protocols.

9.3 Varying efficiencies and dark counts

The first imperfections to be varied were η_{det} and η_{read}. A variable $\eta = \eta_{det} \cdot \eta_{read}$ was used to illustrate the effect on the performance of the modified Jiang protocol.

To begin fidelity and time were plotted as a function of p for different values of η. The parameters used were $L = 1000$ km, $n = 3$, $p_{dark} = 0$ and $dim = 3$. The results can be seen in figure 21 and 22.

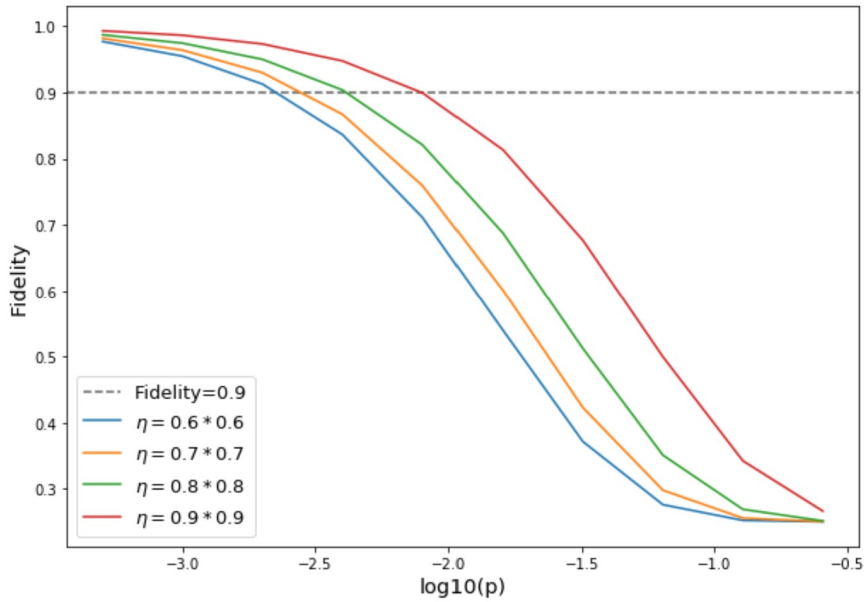

Figure 21: A plot of the fidelity as a function of p. Different values of $\eta = \eta_{det} \cdot \eta_{read}$ were compared. The other parameters were fixed to be $L = 1000$ km, $n = 3$, $p_{dark} = 0$ and $dim = 3$.

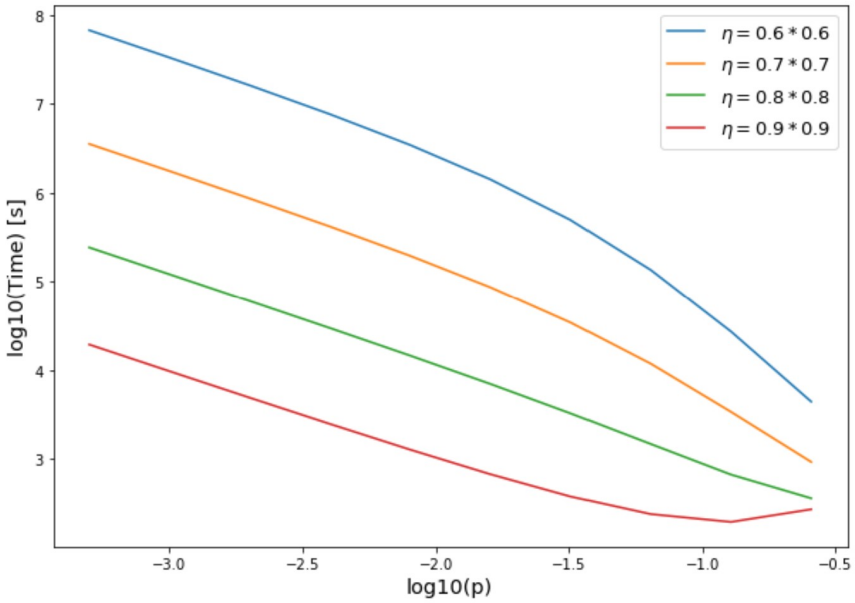

Figure 22: A plot of the time as a function of p. Different values of $\eta = \eta_{det} \cdot \eta_{read}$ were compared. The other parameters were fixed to be $L = 1000$ km, $n = 3$, $p_{dark} = 0$ and $dim = 3$.

One can observe from the figures that not only does a decrease in efficiency make the protocol slower, it also decreases the fidelity of the final state. The time is slower because not reading out an excitation or a photon not being detected can cause no clicks being registered thereby restarting the process. Another possibility is that there is more than one excitation but either one is not read out or it is not detected. This causes the accept of an unwanted state decreasing the fidelity of the resulting state.

The optimal time was calculated for different values of n with same L, p_{dark} and dimension as before. Plotting the optimal time as a function of η resulted in the plots in figure 23.

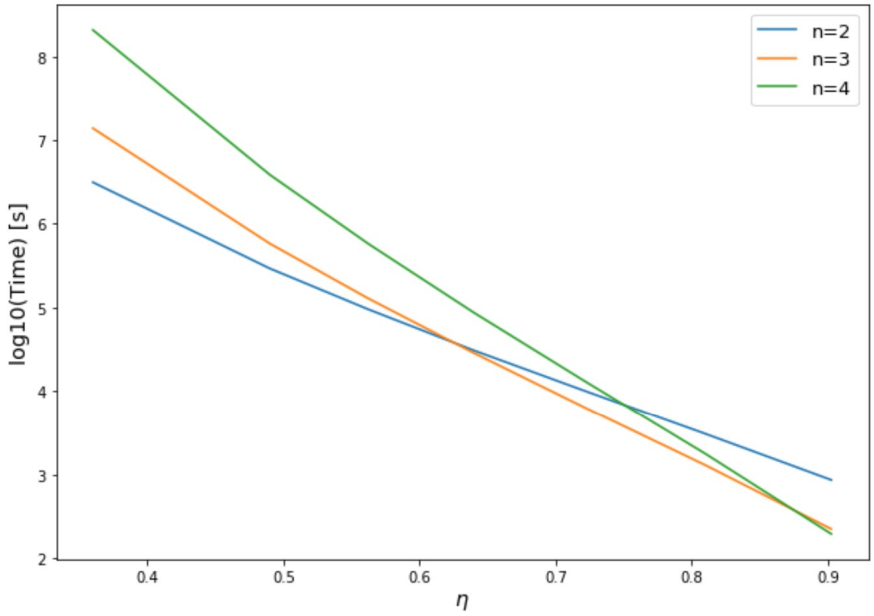

Figure 23: Plot of the optimal time as a function of η for $n = 2$, $n = 3$ and $n = 4$. Other parameters were fixed at $L = 1000$ km, $p_{dark} = 0$ and $dim = 3$.

This plot shows that for low efficiencies less swaps is better. This makes sense considering more swaps means lower fidelity, and the fidelity is already low on low efficiencies.

Though the modified Jiang protocol was shown to be better, it might be interesting to compare the effect of varying the efficiencies on both the standard and modified Jiang protocols for $dim = 3$ and $dim = 2$. The optimal time was plotted as a function of η for $L = 1000$ km, $n = 3$, $p_{dark} = 0$:

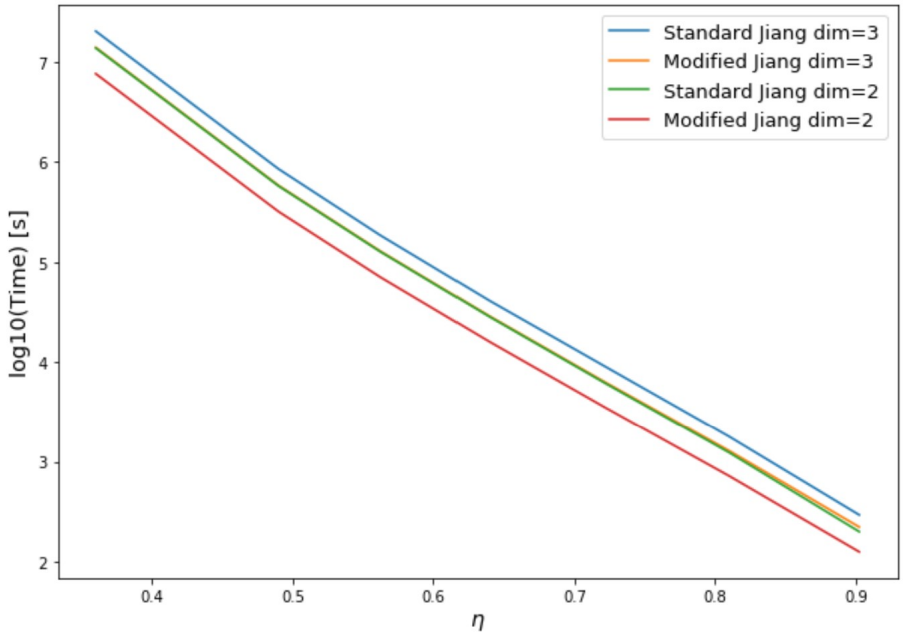

Figure 24: A plot comparing the optimal time as a function of $\eta = \eta_{det} \cdot \eta_{read}$ for the standard Jiang and modified Jiang with $dim = 2$ and $dim = 3$.

We can see the modified Jiang protocol with $dim = 3$ and the standard Jiang protocol are practically equivalent for most values of η. For η around 0.85 they become barely distinguishable.

Then the value of p_{dark} was changed to explore its effect on the modified Jiang protocol.

For $L = 1000$ km, $n = 3$, $\eta_{det} = \eta_{read} = 0.9$ and $dim = 3$ the fidelity and time were plotted for various values of p_{dark}. The results can be found in figures 25 and 26.

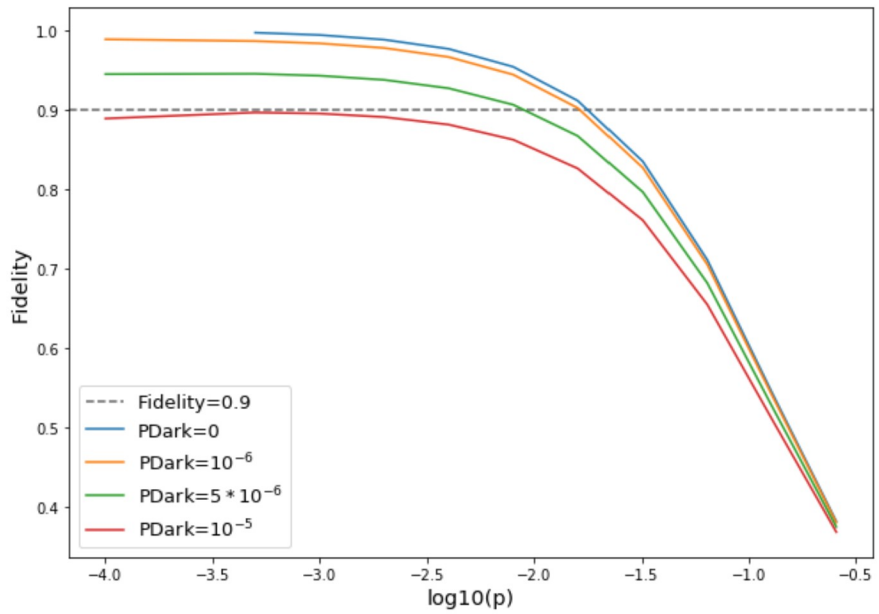

Figure 25: A plot of fidelity as a function of p for different values of p_{dark}.

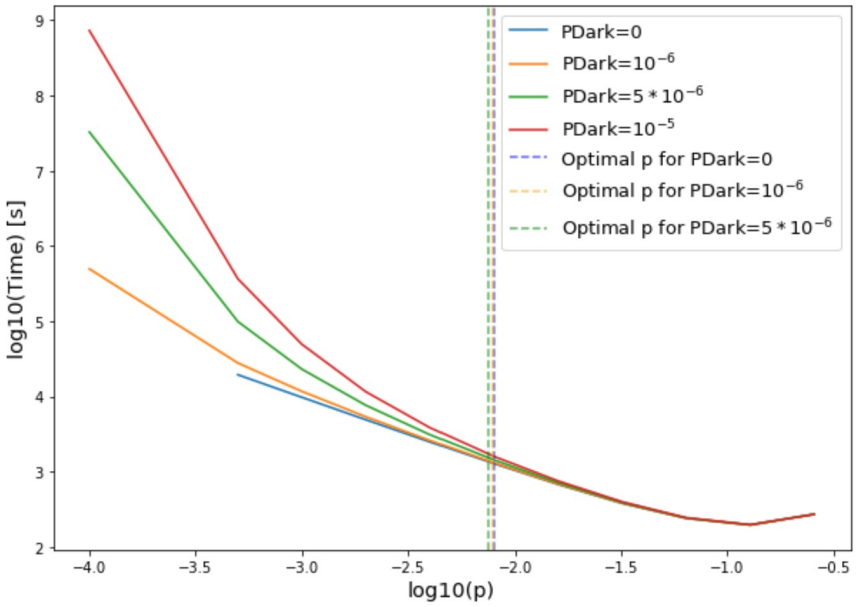

Figure 26: A plot of time as a function of p for different values of p_{dark}.

While a very small probability of dark counts makes little difference the effect increases significantly on both the fidelity and time. For $p_{dark} = 10^{-5}$ it even came to a point where the fidelity never completely reached 0.9 though it came close.

9.4 Suppressing multi-photon errors

A simulation was run where a factor of $\sqrt{x}$ was added to terms where two photons are emitted. As a consequence some terms were modified:

- $p \cdot \eta_t \left|22\right\rangle_{m,ph}$ was changed to $\sqrt{x} \cdot p \cdot \eta_t \left|22\right\rangle_{m,ph}$
- $p^2\eta_t(1-\eta_t) \left|21\right\rangle \left\langle 21\right|_{m,ph}$ was changed to $x \cdot p^2\eta_t(1-\eta_t) \left|21\right\rangle \left\langle 21\right|_{m,ph}$
- $p^2(1-\eta_t)^2 \left|20\right\rangle \left\langle 20\right|_{m,ph}$ was changed to $x \cdot p^2(1-\eta_t)^2 \left|20\right\rangle \left\langle 20\right|_{m,ph}$

Plotting time and fidelity as a function of p for different values of x with the same L, n, η_{det}, η_{read} and $p_{dark} = 0$ produced the graphs in figure 27 and 28.

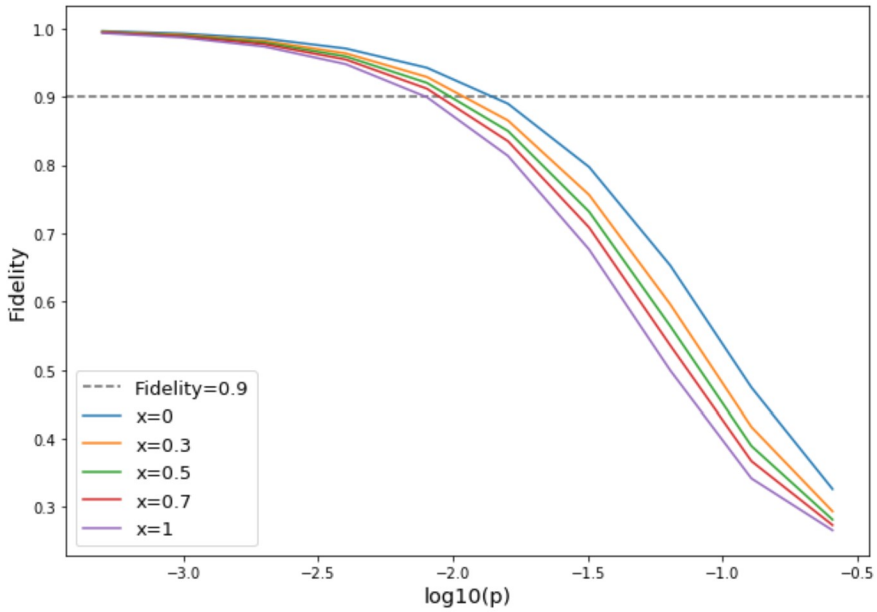

Figure 27: A plot of fidelity as a function of p for different values of x. x is a factor determining the size of the multi-photon error caused by the emission of two photons from the same ensemble.

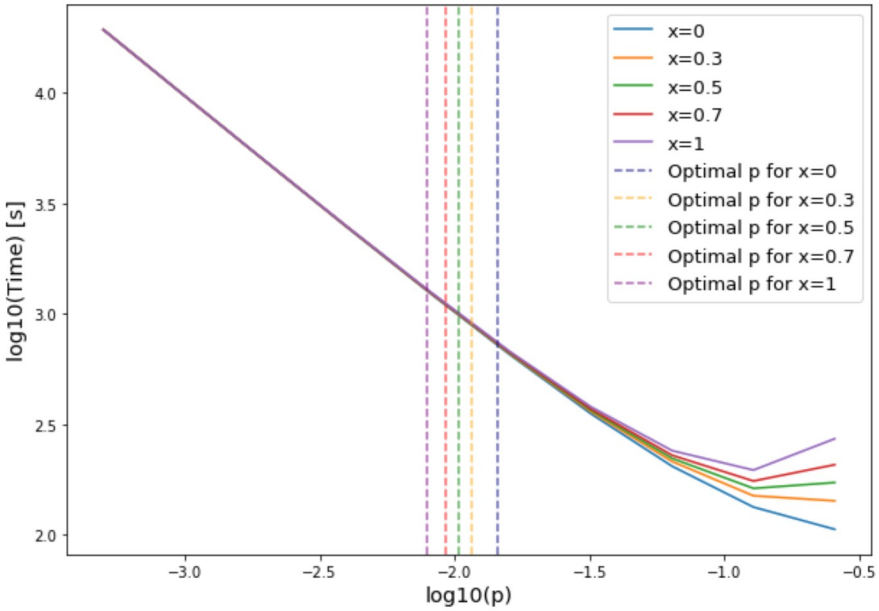

Figure 28: A plot of time as a function of p for different values of x. x is a factor determining the size of the multi-photon error caused by the emission of two photons from the same ensemble.

As one might expect suppressing the multi-photon error term causes an increase in fidelity. Not as much as one may think however. The time remains somewhat the same up to a certain point. After that there is a clear difference as multi-photon errors become more dominant causing increase in time spent for the cases where it was less suppressed.

For different values of n the optimal time for which the fidelity was 0.9 was found for fixed parameters $L = 1000$ km, $\eta_{det} = \eta_{read} = 0.9$ and $p_{dark} = 0$. Plotting the optimal time as a function of x produced the graphs found in figure 29.

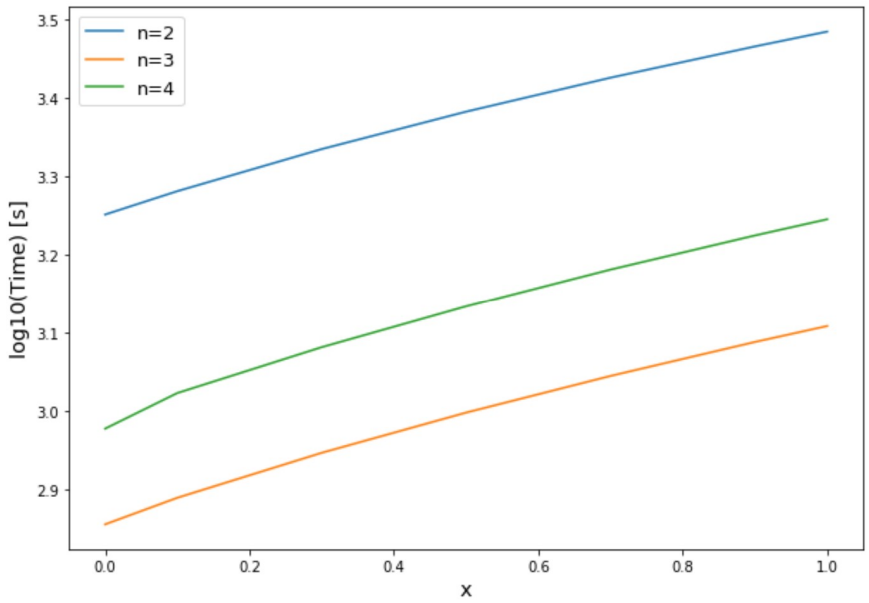

Figure 29: Plot of the optimal time as a function of x for different values of n. x is a factor determining the size of the multi-photon caused by the emission of two photons from the same ensemble.

What this plot illustrates is that regardless of the value of x $n = 3$ is the optimal number of swaps. Note this plot was made for $L = 1000$ km and this might not be the case for other distances. Consider the difference between the point at $L = 5000$ km on figure 9 and 17. For $dim = 2$ $n = 6$ is very clearly better than $n = 5$. For $dim = 3$ it seems $n = 5$ and $n = 6$ cross just before 5000 km. This means there must be certain points for which small values of x have one preferred nesting level and for high values another nesting level is preferred.

9.5 The cost of quantum memories

Quantum memories are costly to make. This means it matters how many memories a repeater protocol requires as the supply of available quantum memories to use is most likely limited.

Suppose 256 memories are available to make quantum repeaters. For a given n it requires 2^{n+2} memories to run the standard or modified Jiang protocol. In other words it would require 16 memories to make a repeater with $n = 2$, 32 to make a repeater with $n = 3$ or 64 to make a repeater with $n = 4$. This means with 256 memories available it would be possible to make 16 repeaters with $n = 2$, 8 repeaters with $n = 3$ or 4 repeaters with $n = 4$. Suppose $n = 3$ is the optimal nesting level. Depending on the distance L it could be that having 16 less optimized repeaters has a higher probability of one of them being successful than the probability of one out of 8 optimized protocols being successful.

For this reason when plotting the optimal time it should be divided by a factor $\frac{256}{2^{2+n}}$ to account

for the fact that for smaller values of n it is possible to make more repeaters.

Plotting the optimal time after it has been divided with the factor as a function of p for different values of n and for $L = 1000$, $\eta_{det} = 0.9$, $\eta_{read} = 0.9$, $p_{dark} = 0$ and $dim = 3$ produced the following plot:

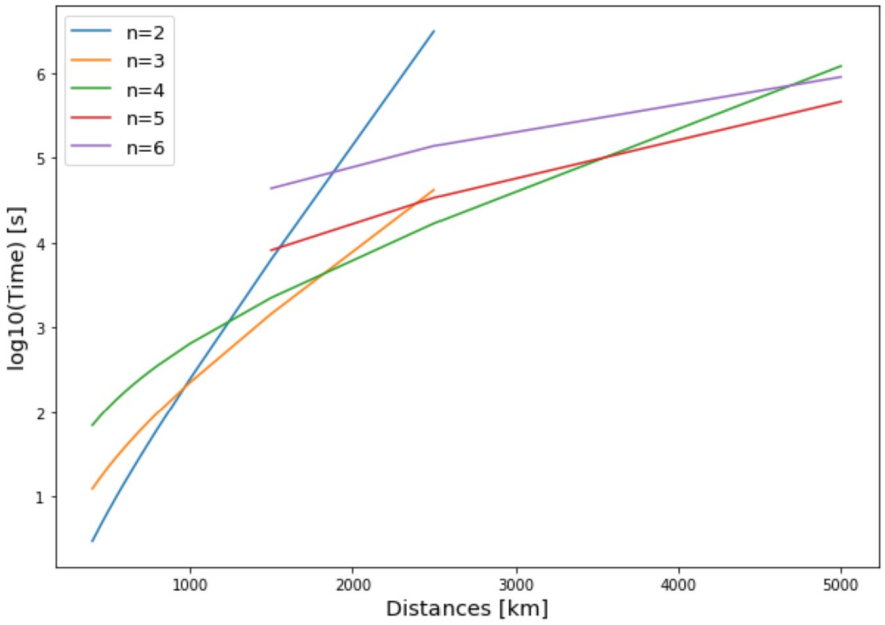

Figure 30: A plot of the optimal time divided by a factor $\left(\frac{256}{2^{2+n}}\right)$ as a function of distance for various values of n.

Compared to figure 17 clearly it takes a longer distance for a higher nesting level to be preferable.

Plotting the optimal time over all n as a function of distance produced the following plot:

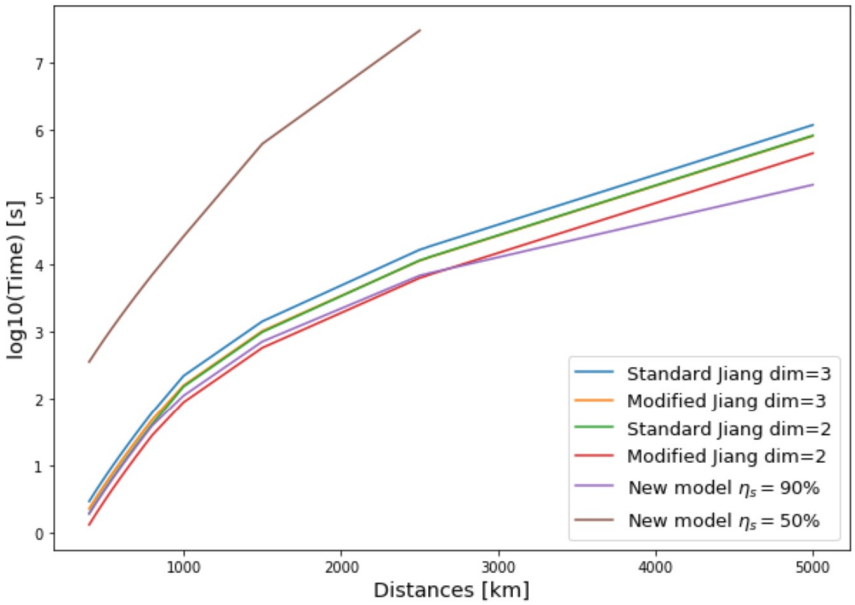

Figure 31: A plot of the optimal time divided by a factor $\left(\frac{256}{2^{2+n}}\right)$ as a function of distance.

Note "New model" was made from data for a model by Anders and Yuxiang (under preparation).

In summary two options can improve the protocol. Removing the multi-photon error from the source emitting two photons and using the modified Jiang protocol instead of the standard Jiang protocol. To quantify the total gain by using both these options the ratio between the standard Jiang protocol with $dim = 3$ and the modified Jiang protocol was calculated. At the point where they were furthest the ratio was 0.379. The point where they were closest the ratio was 0.456.

10 Outlook

Now that we have compared the standard and modified Jiang protocols and looked at the effect of various imperfections this chapter will discuss in greater detail the applications of quantum repeaters.

10.1 What is next?

It could be interesting to explore what happens if the threshold for the accepted fidelity was changed. The choice of a fidelity of 0.9 as the lowest accepted was completely arbitrary, so it could be interesting to explore if requiring a fidelity of e.g. 0.95 would change any of the results significantly.

It is also worth looking into how a repeater would work in an actual communication scheme. To consider a quantum repeater in combination with a subsequent protocol for the actual transmission of information.

10.2 What can quantum repeaters be used for?

Quantum repeaters are a solution to the aforementioned problem of long-distance quantum communication. Repeaters are not yet efficient enough to be useful in an actual communication setting. Either the fidelity of the final state is too poor or the protocol is too time-consuming.

A potential method for improving quantum repeater protocols is multiplexing. The standard Jiang and modified Jiang protocols are well suited for multiplexing. It has been shown [1] that multiplexing can improve the time-cost by as much as a factor of 1250.

However if repeaters can be made efficient enough in the future they open some interesting technological opportunities. For example having a sufficiently efficient way to send information across large distances is a necessary foundation for building a quantum internet.

With a quantum internet quantum cryptography could be implemented to establish secure lines of online communication. It would allow the transfer of qubits which hold significantly more information than the classical bit due to the possibility of superpositions.

11 Conclusion

In summary what this thesis has shown is that quantum repeater protocols are good under ideal conditions. A protocol based on one-click entanglement generation and one-click entanglement swapping only took $2.25 \cdot 10^{-2} s$ for $L = 1000$ km and three swaps. In comparison the probability of successful direct transmission for $L = 1000$ km was only $1.82 \cdot 10^{-20}$ %.

When imperfections were introduced and included the one-click entanglement swapping scheme turned out to be inefficient. It was burdened with a higher time-cost and a decrease in the fidelity of the resulting state. To diminish the effect of imperfections two-click swapping schemes were introduced. As expected the type 1 two-click swap outperformed the type 2 two-click swap as the modified Jiang protocol outperformed the standard Jiang protocol.

Even using repeater protocols that took advantage of the two-click swapping schemes they got slower as well as less accurate i.e. the fidelity of final state decreased. The effect varied between the standard Jiang and the modified Jiang protocol with the modified version being more robust to errors.

In general there was a trade-off in the protocols between fidelity and time. First with respect to p for high values the fidelity was worse whereas the time was shorter. Secondly with respect to swaps the fidelity got worse with more swaps in contrast to the time which got shorter.

To find the optimal time considering these trade-offs the Newton-Raphson algorithm was used. The lowest accepted fidelity was chosen to be 0.9. The optimal time must then be the lowest time still satisfying the fidelity being 0.9 or higher. It was then argued that the p for which the fidelity was exactly 0.9 was also the value of p for which the time was optimal.

Another interesting thing to note was in regards to the optimal time as a function of distance. For longer distances the optimal time was at a higher value of nesting level i.e. higher number of swaps.

The focus of the thesis was exploring the effect of the multi-photon error originating from the probability of a photon source emitting more than one photon. There was as expected an improvement, but it was not as great as hoped. The ratio between the standard Jiang protocol with $dim = 3$ and the modified Jiang protocol with $dim = 2$ was found to be 0.379 when they were furthest and 0.456 when they were closest.

For low efficiencies the protocols not only got slower but the fidelity also decreased. For low probabilities of dark counts the fidelity and the time was barely changed as a function of p. With $p_{dark} = 10^{-5}$ however the fidelity got so low it never completely reached 0.9. The time got significantly worse as well. When varying the effect of the multi-photon error the time remained practically unchanged as a function of p but the fidelity decreased.

Appendix

A Three-particle states

A.1 Three-particle system (bosons)

$$|\Psi_B\rangle = \frac{1}{\sqrt{2}}(\psi_1(r_1)\psi_2(r_2)\psi_3(r_3) + \psi_1(r_1)\psi_2(r_3)\psi_3(r_2) + \psi_1(r_2)\psi_2(r_1)\psi_3(r_3) \tag{A.1}$$

$$+ \psi_1(r_2)\psi_2(r_3)\psi_3(r_1) + \psi_1(r_3)\psi_2(r_2)\psi_3(r_1) + \psi_1(r_3)\psi_2(r_1)\psi_3(r_2)) \tag{A.2}$$

A.2 Three-particle system (fermions)

$$|\Psi_F\rangle = \frac{1}{\sqrt{2}}(\psi_1(r_1)\psi_2(r_2)\psi_3(r_3) - \psi_1(r_1)\psi_2(r_3)\psi_3(r_2) + \psi_1(r_2)\psi_2(r_3)\psi_3(r_1) \tag{A.3}$$

$$- \psi_1(r_2)\psi_2(r_1)\psi_3(r_3) + \psi_1(r_3)\psi_2(r_1)\psi_3(r_2) - \psi_1(r_3)\psi_2(r_2)\psi_3(r_1)) \tag{A.4}$$

B Measurement factors for one-click schemes

B.1 One-click entanglement generation

Table 1: The resulting factors given by the measurement operator $M[i_a, j_a, i_b, j_b] = \sum_{n,m=0}^{2} \alpha(n,m) \cdot \langle\phi|_{ph_a,ph_b}^{n,m} |i_a\rangle\langle j_a| \otimes |i_b\rangle\langle j_b| |\phi\rangle_{ph_a,ph_b}^{n,m}$ ordered according to the state of $|i_a\rangle\langle j_a| \otimes |i_b\rangle\langle j_b|$.

$\|\mathbf{i_a}\rangle\langle\mathbf{j_a}\| \otimes \|\mathbf{i_b}\rangle\langle\mathbf{j_b}\|$	$\mathbf{M}[\mathbf{i_a}, \mathbf{j_a}, \mathbf{i_b}, \mathbf{j_b}]$
$\|0\rangle\langle 0\| \otimes \|0\rangle\langle 0\|$	$p_{dark}(1-p_{dark})$
$\|1\rangle\langle 1\| \otimes \|0\rangle\langle 0\|$	$\frac{\eta_{det}}{2}(1-p_{dark})^2 + (1-\eta_{det})p_{dark}(1-p_{dark})$
$\|0\rangle\langle 0\| \otimes \|1\rangle\langle 1\|$	$\frac{\eta_{det}}{2}(1-p_{dark})^2 + (1-\eta_{det})p_{dark}(1-p_{dark})$
$\|1\rangle\langle 0\| \otimes \|0\rangle\langle 1\|$	$\frac{\eta_{det}}{2}(1-p_{dark})^2$
$\|0\rangle\langle 1\| \otimes \|1\rangle\langle 0\|$	$\frac{\eta_{det}}{2}(1-p_{dark})^2$
$\|1\rangle\langle 1\| \otimes \|1\rangle\langle 1\|$	$\frac{1}{2}(1-\eta_{det}) \cdot 2\eta_{det}(1-p_{dark})^2 + (1-\eta_{det})^2 p_{dark}(1-p_{dark})$
$\|2\rangle\langle 2\| \otimes \|0\rangle\langle 0\|$	$(1-\eta_{det})(\eta_{det}(1-p_{dark}) + (1-\eta_{det})p_{dark})(1-p_{dark})$
$\|0\rangle\langle 0\| \otimes \|2\rangle\langle 2\|$	$(1-\eta_{det})(\eta_{det}(1-p_{dark}) + (1-\eta_{det})p_{dark})(1-p_{dark})$

B.2 One-click entanglement swapping

Table 2: The resulting factors given by the measurement operator $M[m_B, m'_B, m_C, m'_C] = \sum_{n,m=0}^{2} \alpha(n,m) \cdot \langle \phi_+ |_{BC}^{n,m} |m_B\rangle \langle m'_B| \otimes |m_C\rangle \langle m'_C| \phi_+ \rangle_{BC}^{n,m}$ ordered according to the state of $|m_B\rangle \langle m'_B| \otimes |m_C\rangle \langle m'_C|$.

$\|\mathbf{m_B}\rangle \langle \mathbf{m'_B}\| \otimes \|\mathbf{m_C}\rangle \langle \mathbf{m'_C}\|$	$\mathbf{M}[\mathbf{m_B}, \mathbf{m'_B}, \mathbf{m_C}, \mathbf{m'_C}]$
$\|0\rangle \langle 0\| \otimes \|0\rangle \langle 0\|$	$p_{dark}(1-p_{dark})$
$\|1\rangle \langle 1\| \otimes \|0\rangle \langle 0\|$	$\frac{\eta}{2}(1-p_{dark})^2 + (1-\eta)\cdot p_{dark}(1-p_{dark})$
$\|0\rangle \langle 0\| \otimes \|1\rangle \langle 1\|$	$\frac{\eta}{2}(1-p_{dark})^2 + (1-\eta)\cdot p_{dark}(1-p_{dark})$
$\|1\rangle \langle 0\| \otimes \|0\rangle \langle 1\|$	$\frac{\eta}{2}(1-p_{dark})^2$
$\|0\rangle \langle 1\| \otimes \|1\rangle \langle 0\|$	$\frac{\eta}{2}(1-p_{dark})^2$
$\|1\rangle \langle 1\| \otimes \|1\rangle \langle 1\|$	$\frac{1}{2}(1-\eta)\cdot 2\eta\cdot(1-p_{dark})^2 + (1-\eta)^2\cdot p_{dark}(1-p_{dark})$
$\|2\rangle \langle 2\| \otimes \|0\rangle \langle 0\|$	$(1-\eta)\cdot(\eta\cdot(1-p_{dark}) + (1-\eta)p_{dark})\cdot(1-p_{dark})$
$\|0\rangle \langle 0\| \otimes \|2\rangle \langle 2\|$	$(1-\eta)\cdot(\eta\cdot(1-p_{dark}) + (1-\eta)p_{dark})\cdot(1-p_{dark})$

C Extra plots

C.1 Fidelity and time vs. p for dim=2

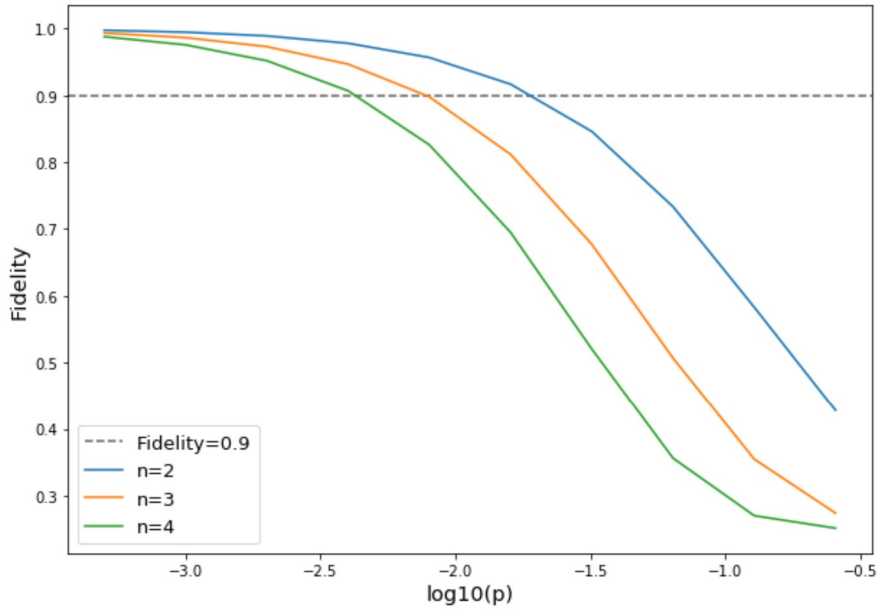

Figure 32: A plot of fidelity as a function of p for different values of n and with parameters $L = 1000$, $\eta_{det} = \eta_{read} = 0.9$, $p_{dark} = 0$ and $dim = 2$. Fidelity decreases with higher p and more swaps.

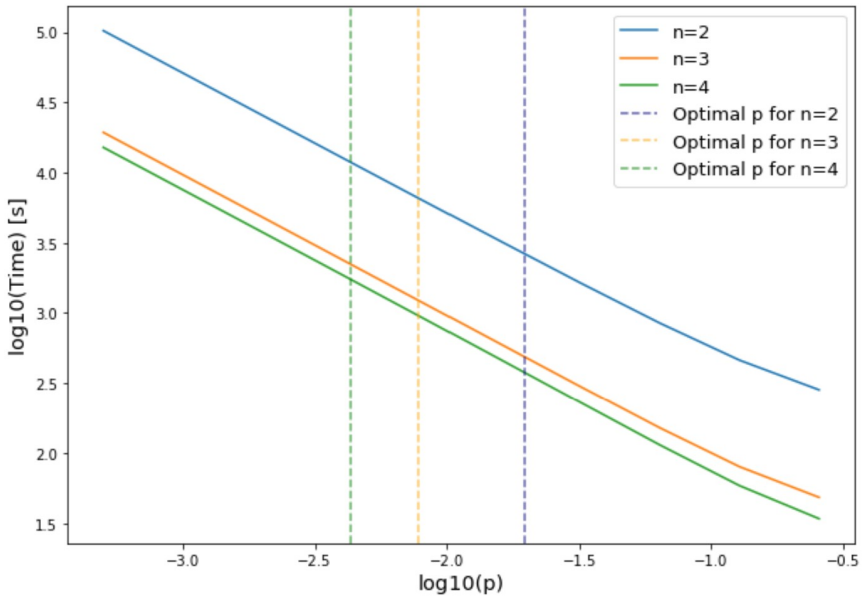

Figure 33: A plot of time as a function of p for different values of n and with parameters $L = 1000$, $\eta_{det} = \eta_{read} = 0.9$, $p_{dark} = 0$ and $dim = 2$. Time is shorter for higher p and more swaps.

C.2 Time vs. p standard and modified Jiang normalized

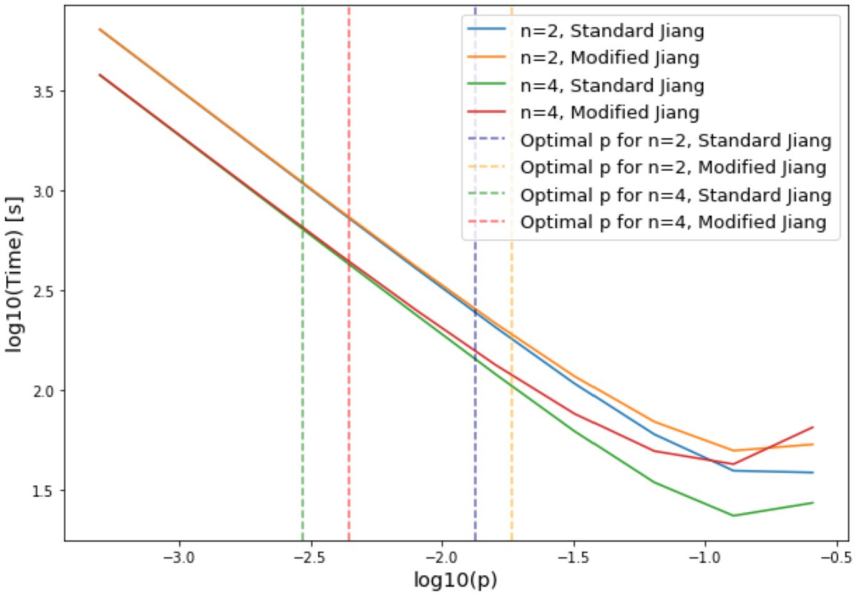

Figure 34: Comparative plots of the time as a function p normalized with a factor dependent on n. Different values of n were plotted for fixed parameters $L = 1000$ km, $\eta_{det} = \eta_{read} = 0.9$, $p_{dark} = 0$ and $dim = 3$.

C.3 Time vs. x comparison of standard vs. modified protocol

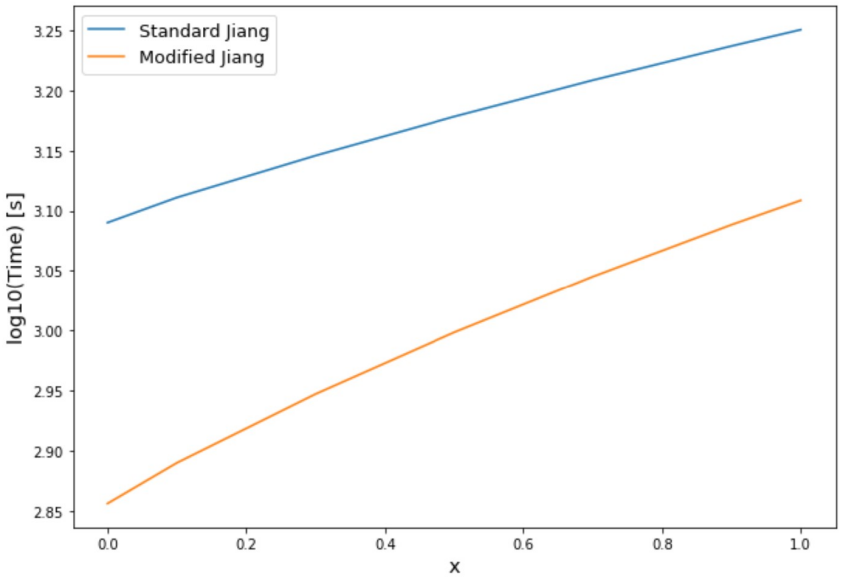

Figure 35: Plot of the optimal time as a function of x for $n = 3$ for the standard and modified protocols.

C.4 Comparison of results with results from Sangouard

In the article [4] in figure 18 is a plot comparing different quantum repeater protocols. Curve C represents the results for the standard Jiang protocol. Comparing these results found by Sangouard with the results from this thesis for the standard Jiang protocol the following comparison was made:

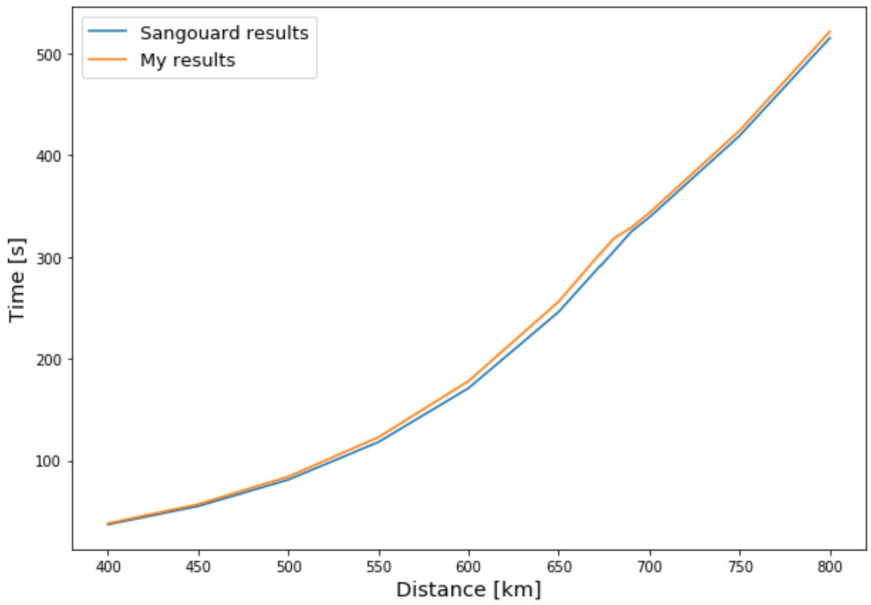

Figure 36: Comparison of the results from the paper by Sangouard et. al. with the results from this thesis.

When the curves are closest the ratio is 0.988. When they are farthest the ratio is 0.960.

The optimal times found seemed to agree well, but the fidelity was found to be less than 0.9. This was explained by the fact that fidelity could have been calculated differently.

The fidelity seemed to agree with the results from [5], but the times were off. This is explained by the fact that the formula used to calculate the time was not well derived at that time.

References

[1] S. C. Wein, J. C. Loredo, M. Maffei, P. Hilaire, A. Harouri, N. Somaschi, A. Lemaître, I. Sagnes, L. Lanco, O. Krebs, A. Auffèves, C. Simon, P. Senellart, and C. Antón-Solanas. Photon-number entanglement generated by sequential excitation of a two-level atom, 2021.

[2] Henrik Buus and Karsten Flensberg. Many-body quantum theory in condensed matter physics, 2016.

[3] Michael A. Nielsen and Isaac L. Chuang. Quantum computation and quantum information, 2016.

[4] Nicolas Sangouard, Christoph Simon, Hugues de Riedmatten, and Nicolas Gisin. Quantum repeaters based on atomic ensembles and linear optics, 2009.

[5] L. Jiang, J. M. Taylor, and M. D. Lukin. Fast and robust approach to long-distance quantum communication with atomic ensembles, jul 2007.